Concentration gradient detection based on Schlieren optics

Janusz Pawliszyn

Guelph-Waterloo Centre for Graduate Work in Chemistry, Department of Chemistry, University of
Waterloo, Waterloo, Ontario, Canada N2L 3G1

1. Introduction

Many powerful instrumental analytical techniques are based on simple physical principles. Snell's Law, associated with refractive index, and Beer's Law, associated with light absorption, are examples that have allowed the design of robust universal and selective chemical sensors. Schlieren optics, another simple optical phenomenon which has been known for over a century [1], has not yet been explored extensively by analytical chemists. This method is particularly attractive because it provides a response that is proportional to the concentration gradients associated with non-uniform distributions of analytes in the detection volume. Thus, in systems which produce high concentration gradients, Schlieren methods are more sensitive than other more established analytical techniques in which the signal is proportional to average analyte concentrations. At the same time the technique de-emphasizes the slow variation in concentration usually associated with drifts. The method provides additional dynamic information about the system by emphasizing changes in concentration rather than their absolute values. This can result in new methods which explore differences in dynamics between analytical species. In addition, Schlieren techniques are well suited for imaging studies to describe the distribution of concentration gradient profiles in the detection volume.

In this review emphasis will be placed on a discussion of the principles behind Schlieren optics methods, including recently introduced selective techniques and the applications relevant to the field of analytical chemistry. Initially, a comparison will be made between concentration gradient methods (gradient methods) and methods that employ the average analyte concentration in the detection volume. This will be followed by a description of the theory and experimental details of Schlieren optics sytems. Finally, there will be an overview of the analytical applications of this technique explored to date.

2. Gradient Versus Concentration Methods

The difference between methods that measure concentration gradient rather than the average concentration of an analyte in the detection volume is illustrated in Fig. 1 for a single dimension. At a given distance x_0, the gradient signal is proportional to $(dc/dx)_{x_0} = \tan\alpha$ while the concentration signal is $C(x_0) = C_0$ respectively (Fig. 1a). If the entire concentration profile is to be characterized by the gradient method, the function obtained will correspond to the derivative of the concentration profile from Fig. 1a. A continuous change in concentration (drift) will be converted to an offset by application of the gradient approach (Fig. 1b). The offset magnitude is dependent on the slope of the drift. In a limiting case, when the step concentration change occurs at x_0, the gradient signal becomes large at this dimension (Fig. 1c). In an ideal situation $(C(x) = H(x_0))$ the gradient signal is infinity $(dC/dx = \delta(x_0))$ even at very small difference in concentration at x_0 and then returns to baseline while the absolute level of the concentration permanently changed. In practical cases however, the signal is dependent on both the magnitude of change as well as the distance over which the change occurs. The quantitative relationship varies depending on the concentration profiles and is briefly discussed below for two important cases.
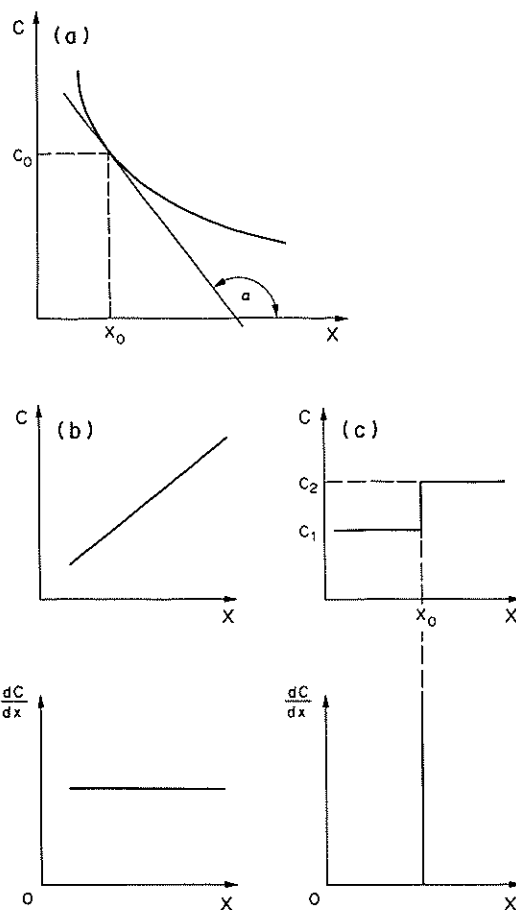
Fig. 1. Concentration vs. gradient measurement. (A) Concentration gradient signal at x_0. (B) Concentration and gradient signals for a constant slope (drift). (C) Concentration and gradient signals for a step change in concentration at x_0.

Gradient detection offers several advantages over the measurement of average concentration. These can be described as the sensitivity advantage, drift reduction and resolution enhancement.

2.1. Sensitivity advantage

It is clear from the above discussion that gradient techniques must be used together with processes which generate "steep" concentration profiles to exhibit high sensitivity. Inherently high concentration gradients are produced in many common analytical methods. One example is the gradient above an electrode surface [2, 3]. The single dimension concentration profiles of analyte A consumed (Fig. 2a) and product B produced (Fig. 2b) during a redox process in a diffusion-controlled potential step experiment are illustrated in Fig. 2. The profile can be described mathematically in terms of error functions depending upon the distance from the electrode and time t following the oxidation or reduction step [2]:

$$C_A = C^\circ \text{erf} \left(\frac{x}{2(Dt)^{1/2}} \right) \tag{1}$$

$$C_B = C^\circ \text{erfc} \left(\frac{x}{2(Dt)^{1/2}} \right) \tag{1a}$$

where C° is an analyte concentration in the bulk and D is the diffusion coefficient of the analyte and product (assuming that $D_A = D_B = D$) in the electrolyte. In these
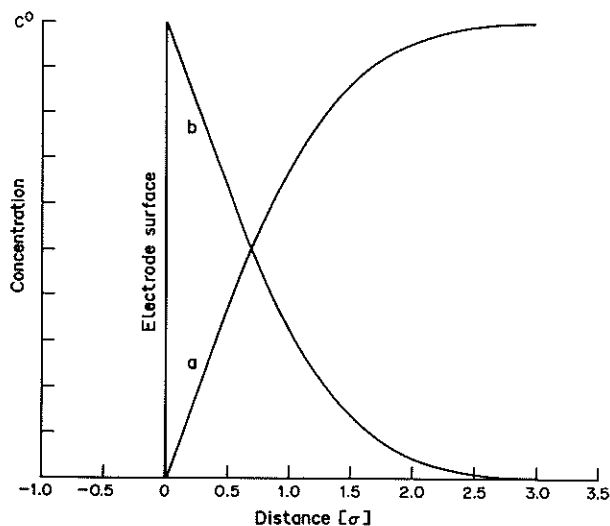
Fig. 2. Concentration profiles of reactant (a) and product (b) above the electrode surface. The distance from the electrode surface is expressed in $\sigma = (2D_R t)^{1/2}$ units. Adapted with permission from Ref. [36].

expressions erf(x) and erfc(x) are the error function and its complementary function respectively. The gradients of analyte concentration versus x are given by the first derivative of the function in Eqn (1):

$$\frac{dC_A(x,t)}{dx} = \frac{\exp(-x^2/4Dt)}{(\pi Dt)^{1/2}} C^\circ. \tag{2}$$

The maximum of the gradient for a given distance x_0 from the electrode surface is produced at time $t = \dfrac{x_0^2}{2D}$ after the beginning of the pulse:

$$\left(\frac{dC_A}{dx}\right)_{x_0}^{max} = \frac{\left(\dfrac{2}{\pi e}\right)^{1/2}}{x_0} C_0 = A_0 C_0. \tag{3}$$

This relationship clearly indicates that the concentration gradient at distance x_0 from the electrode surface is proportional to the concentration of the analyte in the bulk. Additionally, the proportionality constant A_0 is a function of $1/x_0$ and therefore is large when it is evaluated at distances close to the electrode surface. Thus, an analytical method capable of probing the gradient of the concentration close to the electrode surface, should have a high sensitivity in addition to a response that is proportional to the analyte concentration in the bulk. The advantage of the gradient method over concentration methods is particularly evident when the concentration profile of the analyte, or more importantly products or transient species, need to be characterized close to the electrode surface. The concentration gradient magnitude approaches infinity in the vicinity of the surface (see Eqn (3)) while the concentration of the electroactive species is at the bulk level or even drops to zero in the vicinity of the electrode for the analyte (Fig. 2). Thus a high bulk concentration of analyte is required in order to study the electroactive species using a concentration sensor. The concentration gradient method, on the other hand, is very sensitive when it is able to access volumes close to the surface of the electrode. In addition, the concentration gradient sensor is much better suited to the study of the *dynamics* of electrochemical processes in the diffusion layer. This point can be illustrated by the fact that the sensitivity of the concentration gradient method is highest immediately after the potential step, when high concentration

gradients are produced due to large diffusion (dynamics) across the area closest to the electrode. The concentration method, on the other hand, will exhibit the highest sensitivity a long time after the potential step when a large amount of the electrochemical species has accumulated in the diffusion layer.

Another important type of analytical process, which is able to generate high gradients of concentration, involves sample injection and transport in flowing streams. Examples of such methods include flow injection techniques using small ID tubes and ultra high efficiency separation techniques such as capillary chromatography, capillary electrophoresis and field flow fractionation. An injection plug transported in a narrow bore capillary does not undergo much broadening [4] and produces a "sharp" peak at the detector. The usual shape of the signal resembles the Gaussian curve (Fig. 3c) with the peak height expressed as:

$$C_{max} = \frac{1}{F\sigma_t(2\pi)^{1/2}} M \qquad (4)$$

where F is the volume flow rate, σ_t is the standard deviation of the Gaussian in time units, and M is the amount of sample injected. The formula indicates the proportional relationship between M and C_{max} when σ_t is kept constant. This requirement is fulfilled for a given set of experimental conditions. The spatial gradient of a concentration
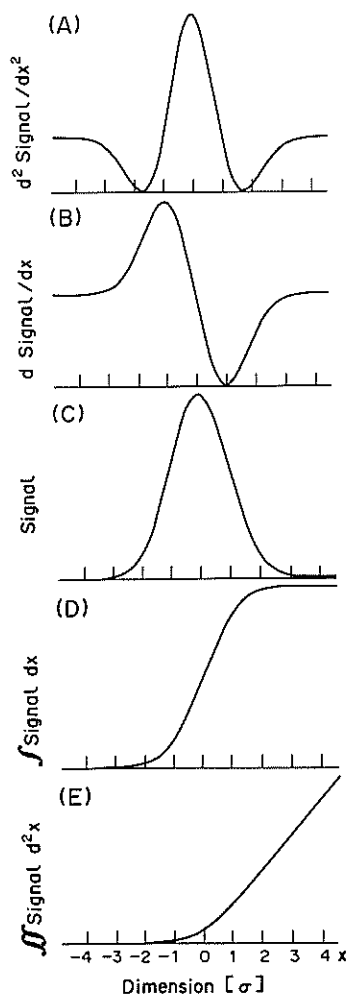

Fig. 3. Signal shapes associated with Gaussian signal profiles: (A) second derivative; (B) first derivative; (C) Gaussian; (D) first integral; (E) second integral. σ—standard deviation of Gaussian.

signal along the direction of flow is a derivative of the Gaussian (Fig. 3b) with the optimum value of:

$$\left(\frac{dC}{dx}\right)_{max} = \left(\frac{dC}{dx}\right)_{\pm\sigma} = \frac{e^{-1/2}}{\sigma_t^2(2\pi)^{1/2}Fv}M = \frac{e^{-1/2}}{\sigma_t v}C_{max} = B_0 C_{max} \quad (5)$$

where v is a linear flow rate. The optimum value for the gradient signal is proportional to the amount of sample injected, M, and C_{max} for a constant σ_t. The ratio of $\left(\frac{dC}{dx}\right)_{max}$ to C_{max}, a constant—B_0, is inversely proportional to the standard deviation σ_t. The more efficient transport process (smaller σ_t), which results in less dispersion of the injection plug, will produce higher sensitivity to the gradient when compared with the concentration detection method. For example, in chromatographic separation, the relative sensitivity enhancement is expected to be a square root of the number of theoretical plates because $\sigma_t = t_r/\sqrt{N}$, where t_r is the retention time [4]. In other words, increased efficiency results in enhanced sensitivity for gradient detection. Additional enhancement can be achieved by taking advantage of the high gradients generated in the radial direction at laminar flow conditions. This is discussed in detail later in the experimental section. If necessary the concentration gradient signal can be converted to concentration versus time by numerical integration. This procedure will transform derivative shape into more conventional peaks.

2.2. Reduction of drifts

Reduction of high-frequency noise when the signal is of low frequency can be accomplished by using low pass filters in either the analog or time domain [5]. A more challenging task involves the reduction of low-frequency noise, such as drift and broad peaks, which often limit the performance of separation methods. For example, it is very difficult to use the refractive index detector in HPLC with solvent gradients. The main difficulty in reducing low frequency drift is that both broad drifts (Fig. 4A–2) and sharp peaks (Fig. 4A–1) contain low frequency information. In other words, it is impossible to filter out drifts without changing the shape of a Gaussian peak. Figure 4 shows broad and narrow peaks in the time and frequency domains. It is clear from Fig. 4B that the frequency range that differentiates sharp peaks from drifts is in the mid frequency range. Broad drifts do not contain information in this region while (Fig. 4B–2) sharp peaks extend to these frequencies (Fig. 4B–1). Any filter that emphasizes mid-range frequencies will eliminate drifts successfully. As noted above, any change in the low frequencies caused by application of such a filter will result in a different signal shape because it will remove some information about the peak. It is important, therefore, to apply a filter that will produce a well-defined signal shape with a magnitude directly related to the concentration of the injected sample.

It is well known that differentiation can reduce drifts substantially. Differentiation in the time domain corresponds to the application of a high pass filter in the frequency (ω) domain [6]:

$$\frac{d^n f(t)}{dt^n} \Rightarrow (i\omega)^n F(\omega) \quad (6)$$

where n is an order of the derivative and $F(\omega)$ is the time output, $f(t)$, described in the frequency domain. For example, the first derivative of the concentration signal in the time domain is equivalent to the linear filter in the frequency domain (Fig. 5a).

Since the concentration gradient method produces signals proportional to the first derivative of concentration, it will reduce drifts substantially by emphasizing sharp changes associated with narrow bands and de-emphasizing broad variations corresponding to drifts.
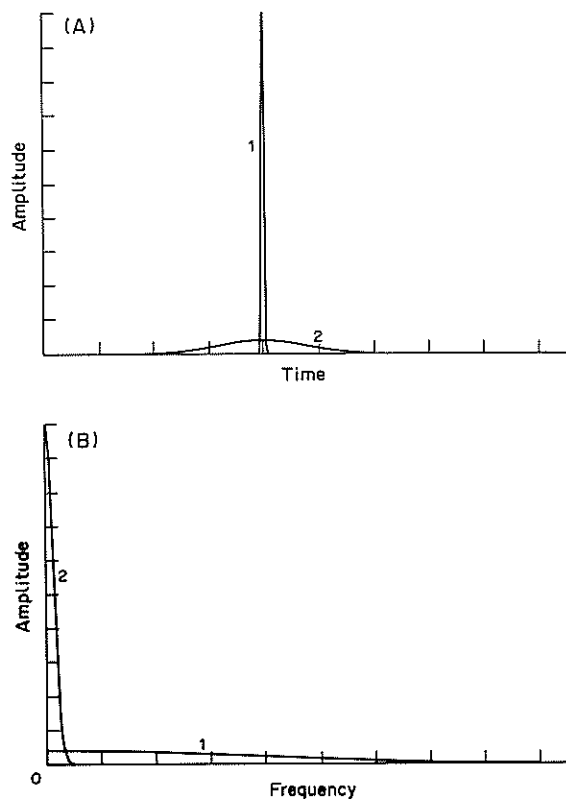
J. PAWLISZYN

Fig. 4. In Gaussian peaks: time (A) and frequency (B) domains; 1, narrow Gaussian; 2, broad
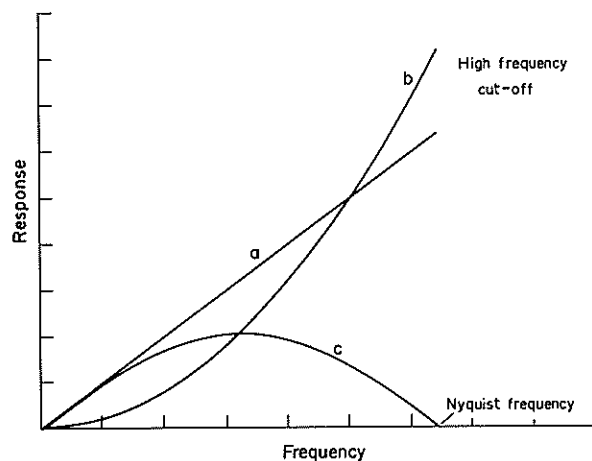Gaussian. Adapted with permission from Ref. [25].

Fig. 5. Frequency response curves for (a) first derivative, (b) second derivative and (c)
differential filters.

2.3. Gradient detection versus differentiation of concentration response

The simplest way to generate a derivative-like response is to apply a mathematical
differentiation of the concentration data. However, this process is not identical to
direct concentration gradient detection. Only under limiting conditions, namely

$$\lim_{\Delta x \to 0} \frac{\Delta C}{\Delta x} = \frac{dC}{dx} \tag{7}$$

are these two functions equivalent. However, since:

$$\lim_{\Delta x \to 0} \Delta C = 0 \tag{8}$$

for the continuous concentration function, it is impossible to produce a good estimate with high spatial resolution of the concentration gradient from concentration data. Indeed small changes in the level of concentration, which are undetectable by the concentration method, can produce high concentration gradients when they occur over a small distance or within a small volume. Thus, important dynamic information about the distributions of the species in a small detection volume is often lost when the concentration rather than the gradient detection method is employed.

The noise-filtering properties of the differential process are substantially different from those in direct derivative or gradient approaches. Let us consider the symmetric differential process:

$$\Delta C(x) = C(x+\Delta x) - C(x-\Delta x), \tag{9}$$

where Δx is a spatial sampling interval. The filtering properties of this approach can be described in the form of a frequency response function (Fig. 5c):

$$F(\omega) = \sin \frac{2\pi}{\Delta x} \tag{10}$$

where $(2\Delta x)^{-1}$, known as the Nyquist frequency, is associated with the acquisition rate. For frequencies at much lower frequencies than $(8\Delta x)^{-1}$, the differential concentration method (Fig. 5c) and direct gradient detection (Fig. 5b) behave similarly. However, as the frequency approaches the Nyquist frequency, a significant difference can be noticed in the filtering properties between both methods. The gradient method progressively emphasizes higher frequencies, while the differential approach attains a maximum at $(4\Delta x)^{-1}$ and then falls to zero at the Nyquist point. Thus, some high frequency information is removed after differentiation. Therefore, the signal after this process has a broader and significantly different shape from the gradient signal collected at the same sampling rate.

2.4. Enhancement in resolution

Figure 5 and Eqn (6) clearly show that taking the derivative of a time-dependent function, such as a chromatogram, results in removal of low frequency information. In the process the chromatographic band is converted into a sharper derivative since slowly varying components of the signal are thereby reduced in magnitude. The net result is a significant enhancement in resolution between closely positioned bands. Figure 6 illustrates the resolution improvement between two Gaussian peaks separated by 3σ ($R = 0.75$) when differentiating the chromatogram. The signals are progressively sharper and therefore better separated from one another. In addition, the change in shape of the signal can facilitate more accurate determinations. For example, the first derivative of a Gaussian peak consists of two peaks separated from one another by 2σ (Fig. 6B). Moreover, the height of each peak is directly proportional to the amount of sample injected into the flowing stream. Therefore, even though the two bands are not fully separated ($R = 0.75$, Fig. 6A), it is still possible to obtain correct quantitative information by measuring the heights of the outside peaks (Fig. 6B). The original concentration signal, however, will not provide (Fig. 6A) an accurate measurement because of the overlap between the two Gaussian peaks. In other words, the gradient method produces a signal which is proportional to the slopes of peaks rather than the heights, as in concentration techniques. The centres of two overlapping peaks are closer to one another than their outside slopes which provides the resolution advantage.
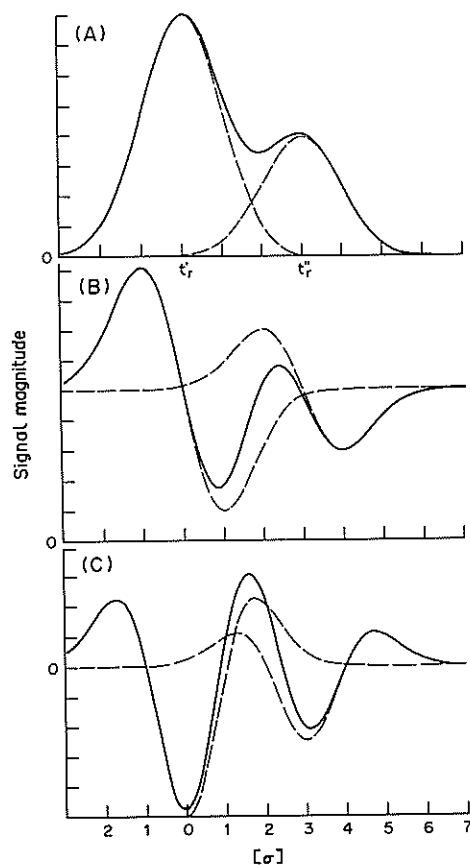
Fig. 6. Improvement in resolution and quantitation of two overlapping peaks during differentiation of concentration response. $t'_r - t''_r = 3\sigma$, where σ is a standard deviation of a chromatographic peak. The ratio of intensities of both peaks is 2 : 1, respectively. (A) Concentration signal; (B) first derivative; (C) second derivative. Broken lines—individual peaks; solid lines—composite signal.

The slope sensitive response of the derivative can provide a test for determining the composition of chromatographic bands. Such methods clearly indicate whether a given peak consists of a single substance or is composed of poorly resolved components. This approach can be used effectively in preparative chromatography to determine the cut-point in order to obtain pure components from partially overlapping bands [7].

The general examples discussed above indicate strongly that in order for any of the concentration gradient methods to be useful in practical applications, they should fulfill a number of specific requirements. In addition to the usual prerequisites such as simplicity and sensitivity, the method of choice should be able to probe small volumes, preferably in a remote fashion, in order not to disturb the system and the high gradients associated with it. For example, these features are necessary if a given method is going to be applied to study electrochemical interfaces or to detect the small volumes of analyte transported through small-bore capillaries. Schlieren optics appear to be ideal for this since the method requires only a single probing light beam to propagate through the detection volume in order to measure the concentration gradients which are present.

3. The Principle of Schlieren Optics

It is well known that the presence of a solute changes the refractive index of the medium [8]. Similarly, concentration gradients formed by the non-uniform distribution of the analyte will provide a corresponding refractive index gradient $\dfrac{dn}{dx} = \dfrac{dn}{dC}\dfrac{dC}{dx}$. The

light propagated through the medium with such a gradient will produce a "streak", or in German a "schliere" [9]. Such an effect can be easily observed when dissolving sugar in water. The physical principle of this phenomenon is illustrated in Fig. 7a. The wavefront (I) of the probing light beam encounters the refractive index gradient at time t. The different sections of this wavefront experience different refractive indexes. Therefore, various parts of the probe beam will propagate through the gradient in the medium with different velocities since the light velocity is inversely proportional to the refractive index n: $v = c/n$, where c is the velocity of light in vacuum ($n=1$). After a time increment dt, the parts of the beam which experience a lower refractive index will propagate further than those in other regions, thus producing a phase shift. This phase difference will result in wavefront II, formed at time $t+dt$, being tilted relative to wavefront I. The net effect will be a deflection of the probe beam towards higher refractive indexes since light similar to other waves always propagates perpendicular to its wavefront.

The quantitative relationship between the deflection angle θ and the detector cell dimension L, assuming a uniform refractive index gradient $\dfrac{dn}{dx}$ normal to the probe beam direction (Fig. 7b), can be derived using Fermat's principle, which states that the light path through the medium is such that the time necessary for its traversal is a minimum [10]:

$$\tan \theta = \sin h \frac{L}{n}\frac{dn}{dx} = \frac{L}{n}\frac{dn}{dx} + \left(\frac{dn}{dx}\right)^3 \frac{L^3}{n^3 3!} + \left(\frac{dn}{dx}\right)^5 \frac{L^5}{n^5 5!} \cdots \tag{12}$$

where n is the refractive index of the medium. For most practical analytical cases where L and θ are small, we can approximate θ by:

$$\theta = \frac{L}{n}\frac{dn}{dx} = \frac{L}{n}\frac{dn}{dC}\frac{dC}{dx} \tag{13}$$
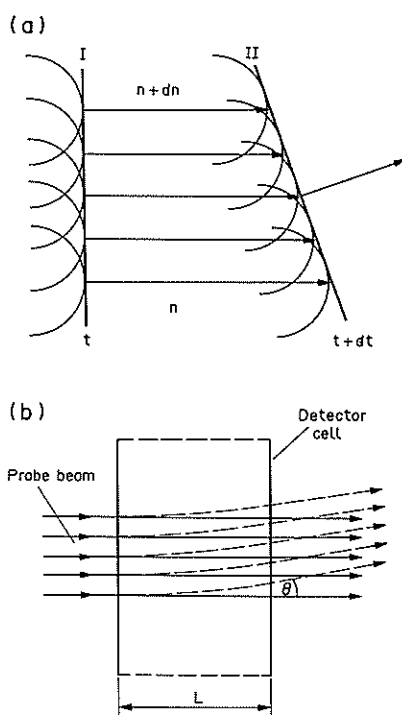
(a)

(b)

Fig. 7. Principle of Schlieren Optics. (A) Tilting of the light waveform propagating through the medium with uniform refractive index gradient and (B) propagation of the light beam through the detector cell without the solute present (solid lines) and through the concentration gradient produced by the eluting peak (dashed lines).

In order to define the concentration gradients from the above relationship all constants must be well characterized. The parameters n and L are associated with the particular experimental design. It is more difficult to assess the proportionality constant dn/dC. In the first approximation it can be estimated by adding specific refractions $\nu = (n-1)/\rho$ where ρ is the density [8]. If we assume that the densities of the medium and the solute are similar, the changes of the refractive index of the medium due to changes in the solute concentration can be expressed as:

$$\frac{dn}{dC} = \frac{M_S}{m_M} (n_S - n_M) \tag{14}$$

where M_S is the molecular weight of a given solute, m_M the mass of one liter of medium with solute, while n_S and n_M are refractive indexes of solute and medium, respectively. The difference, $n_S - n_M$, is usually close to 0.1 for solids and liquids [11]. Therefore, $\frac{dn}{dC}$ can be estimated to $10^{-2}/M$ for solid and liquid media with a solute of low molecular weight ($M_S \sim 100$ g/mol). This coefficient increases in proportion to the molecular weight of the solute.

The simple approximation discussed above assumes a linear relationship between the magnitude of refractive index change and the concentration of analyte in the medium. However, in practice, significant departure from this assumption is observed. A more correct relationship can be derived by starting from the Clausius-Mosotti relation [12] which leads to the relationship [13]:

$$\Delta n \, K_M = \frac{M_S}{m_M} C_S (F_S - F_M)$$

where:

$$F_S = (n_S^2 - 1)(n_S^2 + 2)$$
$$F_M = (n_M^2 - 1)(n_M^2 + 2)$$
$$K_M = 6n_M/(n_M^2 + 2)^2,$$

and therefore

$$\frac{dn}{dC} = \frac{M_S}{m_M} \frac{F_S - F_M}{K_M}. \tag{15}$$

The exact relationship between the concentration of analyte in the medium and the refractive index (and dn/dC) can be measured experimentally. The experimental values should be considered when performing careful analysis of data since in many cases dn/dC deviates significantly from the approximate relationships discussed above. The magnitude of dn/dC is also dependent on the light wavelength used in the experiment and generally increases for shorter wavelengths [15]. In Eqn (13) we assumed a constant concentration gradient along the path of the light beam. If this is not true the integral along L should be calculated:

$$\int_0^L \frac{1}{n} \frac{dn}{dC} \frac{\partial C(L,x)}{\partial x} \, dL \tag{16}$$

4. EXPERIMENTAL ARRANGEMENTS

Many different optical systems have been developed to investigate concentration inhomogeneities using the light deflection phenomenon described above. These methods

are usually referred to as Schlieren optics techniques. The groundwork in developing these systems was done over a century ago by TOEPLER [1] in his investigations of the inhomogeneities present in glass used to manufacture optical components (such as lenses). The inhomogeneities were produced from incomplete mixing of the glass constituents. Some of the methods he applied were similar to those used earlier by FOUCAULT [14] for detecting aberrations in lenses and mirrors. A number of comprehensive reviews have been published since then describing various experimental arrangements related to the application of this optical technique to many important areas of science such as: flow visualization [15], flames [16], electrochemistry, electrophoresis and diffusion [17, 18]. This paper is limited to the most important concepts and new developments in the field which are highly relevant to the application of this phenomenon to the area of analytical chemistry.

4.1. Single probe beam arrangement

Traditionally, the probing light beam in the Schlieren optics method has been generated by an incandescent lamp. The beam is passed through the object in which concentration gradients are found. After some optical signal processing [1, 9, 15–19], the beam is recorded on a photographic plate or on a screen. The change in the intensity distribution across the probing beam represents the refractive index gradient fields present in the object. To provide reasonably good quantitative results, the Schlieren images need to be carefully analyzed using densitometers. This is a lengthy and difficult process. Figure 8A illustrates the simplest, traditional Schlieren optics experiment—a shadowgraph system [15, 16]. The sensitivity and resolution of this simple method is very poor. The overall change in light density registered on the screen is produced as result of a sum of local deflections which occur as the light beam crosses the object. Since the diameter of the beam is large, the assignment of the deflection signal to a particular area is difficult. Analysis of the results gives essentially an integral of the refractive index gradient associated with the object as a whole. Further, the sensitivity of such a deflection measurement is very low since detection of the change in light intensity distribution relies on photographic plates or screens. For these reasons, Schlieren optics found only a limited number of quantitative applications in analytical chemistry [17, 18].

This situation can be dramatically improved by using modern optical and communication technology. For example, the incandescent lamp can be replaced by a laser with
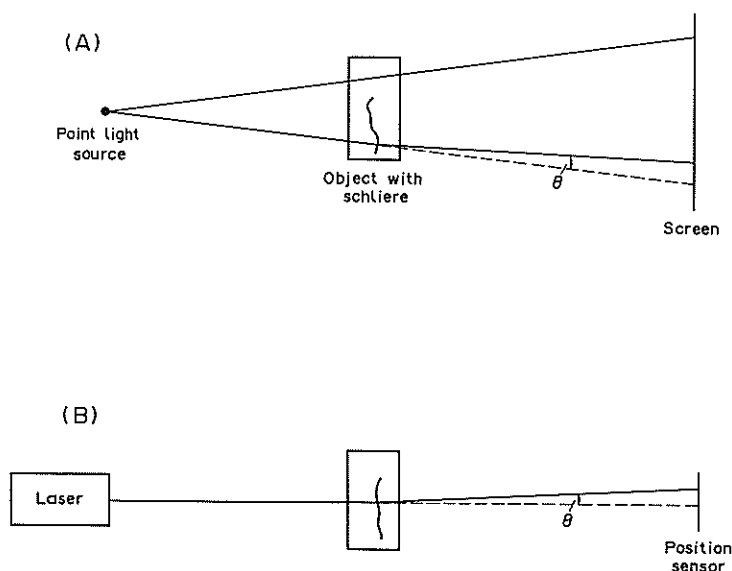

Fig. 8. (A) Example of a traditional Schlieren optics arrangement, shadowgraph system, (B) modern laser beam deflection system.

a collimated beam and the screen by a silicon position sensor (Fig. 8B). In this arrangement a well-defined, small cross-sectional area between the object and the laser beam is probed. In addition, modern light position detection technology, which uses inexpensive silicon photodiodes, allows detection angle measurement down to 10^{-9} rad [20, 21].

Figure 9 shows the schematic of a typical single-dimension sensor in more detail. It consists of a laser, lens, analysed object and the position sensor. The most widely accepted way of measuring the deflection of the laser beam is to use two photodiodes placed close to one another (Fig. 9B). Initially, the position of the beam is adjusted to ensure that the centre of its intensity profile points to the area between two sensors (Fig. 9, solid lines). In this position, both photosensitive surfaces are irradiated uniformly and both photodiodes generate the same photocurrent. If the beam is deflected during the experiment, the amount of light energy falling on both diodes will be unequal since the intensity profile will shift with respect to the stationary detector (Fig. 9, broken lines). The difference between photocurrents (Δi) associated with the photodiodes corresponds to the position of the laser beam in the detector plane relative to the null position. The difference in the current is proportional to the change in position (Δa) for small deflections (α) where $\tan \alpha = \Delta a/M$ (1) and M is a distance between the object and the detector. The sensitivity of the light position measurement can be expressed as:

$$\Delta i = 2\Delta I K \tag{17}$$

where ΔI is the change of the light intensity (W) reaching one photodiode, K is the light conversion efficiency (A/W) and the factor 2 is present because the increase in intensity at one photodiode produces the same decrease in intensity at the other photodiode and therefore the difference is doubled. The change in light intensity falling on a photodiode, expressed as a fraction of total intensity falling on the sensor, is proportional to the ratio of the shaded area of the beam intensity (Fig. 9) to the total area of the beam at the detector plane. This assumption is valid for a centrosymmetric distribution of light intensity across the beam such as the Gaussian profile characteristic for lasers and when there are small deflections in comparison with the beam diameter. Therefore:

$$\frac{\Delta I}{I} = \frac{\Delta a}{\frac{\pi a^2}{4}} = \frac{4}{\pi} \frac{\Delta a}{a} \tag{18}$$

where I is the intensity of the probe beam, and a is a diameter of the beam in the detector plane.

Using Eqns (17) and (18) and since
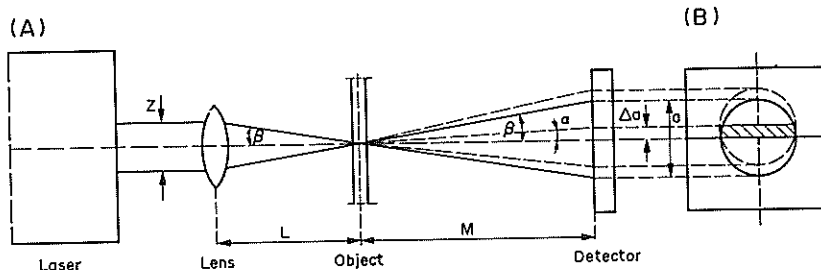
$$a = 2M\tan\beta = Z\frac{M}{L} \tag{19}$$

Fig. 9. Laser beam deflection system in more detail. Z—diameter of laser beam; M—distance of the object from detector; a—diameter of the beam at the detector surface; Δa—shift of the laser beam in the detector plane; α—deflection angle.

where L is the focal length of the lens and β is the beam divergence angle, the sensitivity of the measurement can be expressed as:

$$\Delta i = 2K\Delta I = 2K \frac{4}{\pi} I \frac{M\tan\alpha}{ZM} L = \frac{8}{\pi} KI \frac{L}{Z} \tan\alpha. \tag{20}$$

For very small deflection angles (α) we can estimate:

$$\Delta i = \frac{8}{\pi} KI \frac{L}{Z} \alpha. \tag{21}$$

Equation (21) indicates that to obtain a highly sensitive deflection measurement, sources which produce narrow, collimated and high intensity beams should be used. The beams should not be focused unless necessary and, if required, the longest possible focal length lens should be used. The high spatial resolution will require tight focusing of the beam. Therefore, careful optimization of the optical system is necessary for each application. Equation (21) clearly indicates that the sensitivity of the measurement is independent of the distance between the object and the detector for the same optical arrangement (Z and L). However, it is only true if two photodiodes are very close to one another so that the dividing area between them is negligible by comparison with the diameter of the beam.

4.2. Simple electronic transducers

Several electronic circuits can be used to measure the difference in currents produced by the two photodiodes. The simplest one, based on a single operational amplifier, is shown in Fig. 10. The output voltage in this configuration is proportional to the differential current between the two photodiodes entering the feedback loop. This simple circuit requires two independent, electronically isolated photodiodes [22]. Often, two photodiodes located on the same substrate are used as position sensors (bicell configuration). In such a case, the two photodiodes have a common cathode and therefore require conversion of the photocurrent from each diode to a voltage before subtraction of the appropriate voltage.

The deflection of the light beam can also be measured using lateral sensors. These silicon components are capable of producing a signal proportional to the position of the beam over a large distance—sometimes over a few centimeters. However, their sensitivities are substantially lower compared to the method involving two separate photodiodes and they are generally more expensive.

4.3. Sources of noise

The main source of fundamental noise in the measurement of light position is the shot noise associated with the high level of photocurrent produced by the high intensity light source irradiating the detector. This noise level is only approximately 10^{-10} rad/ $\sqrt{\text{Hz}}$ [21]. This allows highly sensitive detection in narrow band, high frequency
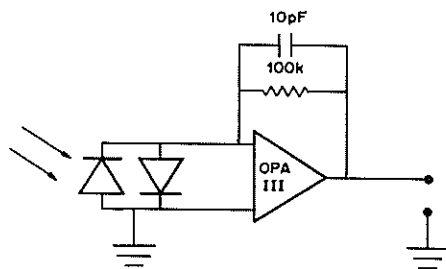
Fig. 10. The electronic design of a simple position sensor. OPA-111 was supplied by Burr Brown, Tucson, AZ and the photodiodes were supplied by Hamamatsu Corporation, Bridgewater, NJ. Adapted with permission from Ref. [22].

measurements. For low frequency measurements, such as the monitoring of the slowly varying gradients produced in flowing streams, electronic flicker noise is expected to be significantly higher than the fundamental component. This type of noise can be eliminated by modulating the probe beam and using lock-in detection. This process will move the measurement to higher frequencies and will enable narrow band width measurement. In practice, however, the slowly varying instabilities of the light beam, such as beam drifts and intensity fluctuation, limit the sensitivity of the deflection measurement [22]. These latter sources of noise are strongly dependent on the type of light source producing the probe beam. Hence, the sensitivity of Schlieren systems is related to the source used. For example, low frequency pointing noise is greatest for a He–Ne laser (10 μrad), moderate for laser diodes (1 μrad) and the best for light emitting diodes (80 nrad). Similarly, intensity fluctuations are highest for the He–Ne laser and correspond to 0.1% of total intensity, while for the solid state light sources they are only 2×10^{-5} fraction. It should be emphasized that these sources of noise are significant only at low frequencies. For high frequencies the shot noise limit can be achieved. However, in Schlieren optics measurements, where slow changes in the refractive index gradient are monitored, the latter components of the noise are the limiting factors.

4.4. Optical arrangements

As pointed out above, there is an advantage to using semiconductor light sources, particularly LEDs. However, they do not produce highly collimated light beams and, therefore, focusing on small objects becomes very difficult. The optimum solution to this situation is to couple the LEDs into small diameter, optical fibers (preferably single mode fibers) and then use the fibers to irradiate the object being investigated. Figure 11 illustrates such a design for detecting solutes flowing through a cross-connection [23]. The probe beam was produced by a light-emitting diode coupled onto a 50 μm optical fiber. Similarly, the silicon detector was coupled to a 200 μm core optical fiber. Both optical fibers were located at opposite sides of a cross-connection in the off-centre position so that only part of the emitted light reaches the photodiode. The collection efficiency of the detector fiber is dependent on the deflection angle of the probe beam produced by concentration gradients in the cell. Figure 11b shows a simple electronic circuit that can be used to monitor the eluting solutes [23].

Another interesting alternative is to use laser diodes, particularly the recently introduced, inexpensive, small devices emitting at 670 nm. Compact collimating optics and power supplies are also available. The light from these sources can be focused to a spot of a few microns in diameter.

In comparison to semiconductor devices, gas lasers such as the He–Ne laser have a much better collimated beam and therefore allow more efficient direct focusing of the beam into small systems such as capillary tubes. However, careful consideration of the detection system is required in order to reduce the effect of large, low frequency, position and intensity noise on refractive index gradient measurements. Figure 12 shows various detection schemes involving single cell, bicell and quadrant silicon detectors. Intensity fluctuations are only significant when a single detector is used (Fig. 12B, E, F). Even in this situation this noise can be reduced significantly by applying a reference photodiode. In such an optical arrangement the beam splitter is used to divert a portion of the energy onto the reference detector. The output from the position sensor is divided by the reference signal to compensate for intensity fluctuations. In the case of two photodiode systems (Fig. 12A, C, D) one photodiode, in fact, works as reference to the other. Even simple signal processing circuits (for example, Fig. 10), are able to reduce the effect of the intensity fluctuation on the beam deflection measurement when the outputs are subtracted without additional division. This is especially true if the beam is initially well positioned between the two photodiodes. The precision of the measurement in this situation corresponds to the magnitude of the laser intensity fluctuation as a fraction of total power (0.1% for the He–Ne laser).
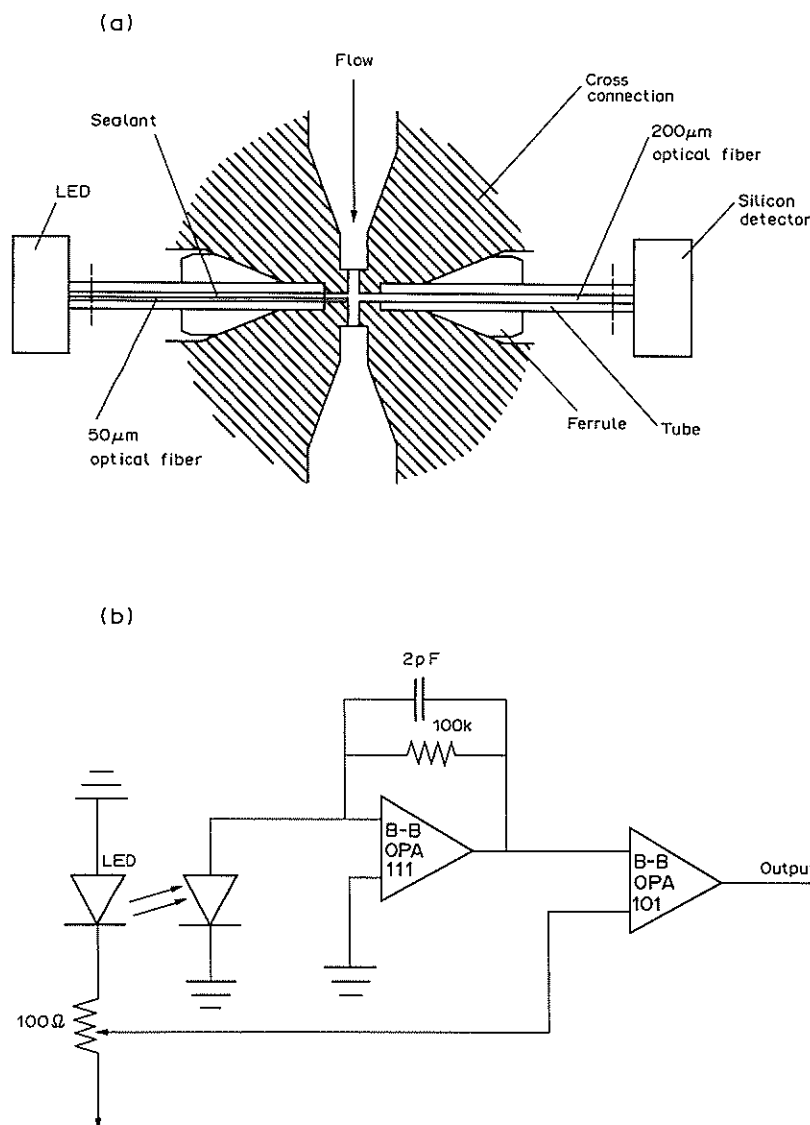
(a)

(b)

Fig. 11. Example of the concentration gradient detector design using LED and silicon detectors coupled to optical fibers fitted into a chromatographic cross connection: (a) geometrical configuration and (b) electronic circuit. Adapted with permission from Ref. [23].

The precision cannot be significantly improved by introducing additional division [24] unless very expensive high precision components are utilized.

A more important challenge in the light deflection measurement is the pointing noise of the laser beam. One way to reduce the effects of this noise is to use a differential arrangement based on two equivalent beams generated by the same laser source. An example of such a system is shown in Fig. 13. The focal length of the system is determined by the relative distance between two lenses [24]. This system can be used in a parallel differential arrangement. One of the beams propagates through the capillary that contains the sample, and the other one through the reference capillary filled with the solvent. A single quadrant detector with associated electronics can be used to monitor the difference in deflection between the two beams, this difference is related to the refractive index gradients produced by the sample components (Fig. 12C).

The other way of effectively using the optical system from Fig. 13 to reduce position drifts is sequential arrangement [25]. Both beams are focused into the detection volume close to one another. The difference in deflection between the two beams is determined
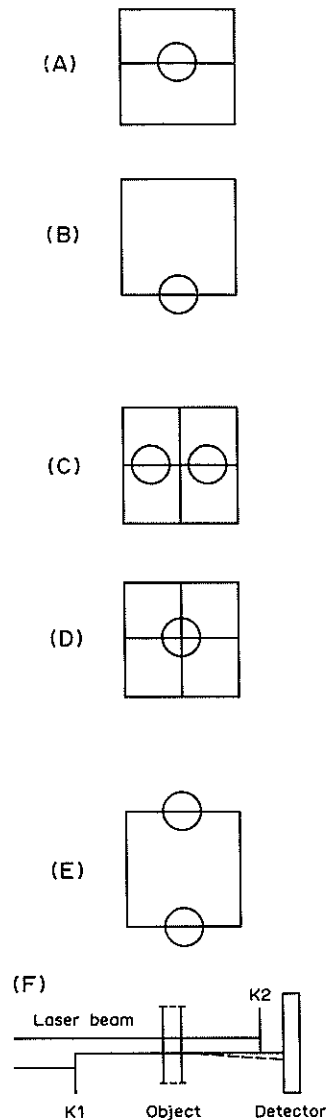
J. PAWLISZYN

(A)

(B)

(C)

(D)

(E)

(F)

K2

Laser beam

K1   Object   Detector

Fig. 12. Detection of laser beam position with (A) bicell; (B) single silicon photodiode; (C) quadrant detector in differential mode; (D) quadrant x–y detection; (E) sequential differential detection using single photodiode; (F) dark background Schlieren optics arrangement with two knife edges and low dark current detector.

by a single photodiode (see Fig. 12E). Each beam irradiates only a part of the photodiode active area. One of the beams is split in half by the upper edge of the photodiode while the other is split by the lower edge. Any change in position of the laser beam affects both beams to the same degree, but the net signal (photocurrent) generated by the detector will not change. For example, if both beams move upward simultaneously the net change of light flux reaching the detector is unchanged because the loss produced by translation of the upper beam is compensated by the movement of the lower beam. This optical system compensates not only for the pointing instability of the laser, but also for any mechanical vibrations and temperature gradients that might occur in real detection devices [25].

The other method which can be used to reduce the position noise is shown in Fig. 12F. This scheme is related to the Schlieren-Toepler arrangement, which will be discussed later [9]. This method applies two knife edges. One is used to introduce a sharp change in light intensity and is located in front of the object. The other edge eliminates the second part of the light beam after it has passed through the object. If
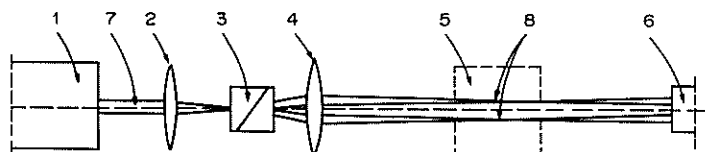
Fig. 13. Schematic of the dual beam position sensor. (1) Laser head; (2), (4) lenses; (3) Wollaston prism; (5) sample; (6) detector; (7) laser beam; (8) focus points of the probe and reference beams.

refractive index gradients or other sources of light deflection are not present in the object, no light reaches the detector. However, if the beam is deflected downwards, significant amounts of light will reach the detector and produce a signal. The most significant limitation of such a system is its ability to detect deflection in one direction. In some cases, the direction of the light deflection associated with the concentration gradient is of interest. A quadrant detector (Fig. 12D) can be used to measure the direction of the gradient.

Most of the detection methods illustrated in Fig. 12 use the relative amount of light reaching the photodiodes as the means of detecting the beam position; therefore, any non-uniform changes of the system which produce a loss in the intensity of the probe beam will be indistinguishable from the deflection signal corresponding to the refractive index gradient. For example, if the probe beam is absorbed by an analyte, non-uniform changes in the light intensity corresponding to the concentration profile are produced. The scattering of light by particles or micro-bubbles present in the system will produce a similar effect. These artifacts can be easily detected by monitoring the total amount of light reaching the photosensor. The refractive index gradients only produce the deflection of light without intensity change while the interferences mentioned above partially extinguish the beam.

4.5. Multidimensional studies

Schlieren optics, in addition to detecting a concentration gradient in one dimension along the probing light beam path, can also be used to image the gradient fields. In fact, Schlieren methods are used widely to study plasma dynamics, flames and flow profiles [15, 16, 26]. The simplest experimental method, the shadowgraph technique [26], is to pass the light beam through the object and monitor the intensity profile before the gradient field is generated when it exists and after it has ceased. On the basis of change in the light intensity distribution, and by applying intensive calculations using ray tracing methods, one can follow the evolution of the phenomenon involving concentration gradients [15, 16, 27]. In this technique the intensity distribution at the detector plane is proportional to the second derivative of the concentration distribution in the object. Figure 14 illustrates this relationship for a shadowgraph produced by a Gaussian peak formed by a solute. In the absence of the gradient field the detection
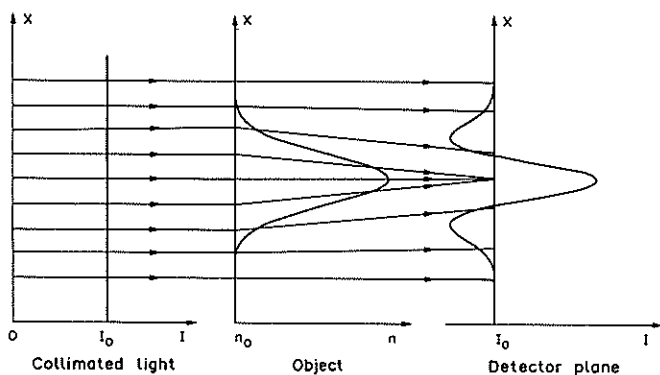

Fig. 14. Principle of the shadowgraph imaging method, illustrated for the Gaussian shaped refractive index field.

plane is irradiated by uniform intensity. On Fig. 14 this occurs in the areas away from the peak where rays propagate through the object unaffected by the gradients. However, the rays which propagate through the concentration profile of the Gaussian peak undergo deflection due to the inhomogeneous refractive index field. If we assume that the refractive index of the solute is higher than that of the medium then the deflection of the light will be directed towards the center of the peak where the highest refractive index is present. This effect will result in higher light intensity in the center of the image followed by decrease away from the center. The generated intensity profile will correspond to the second derivative of the Gaussian peak. On the basis of this discussion it should not be surprising to observe the second derivative response by using two closely propagating beams placed in a sequential deferential arrangement [25].

Much more optically complex, yet simple in analysis, is the system first described by FOUCAULT [14] and TOEPLER [1] and illustrated on Fig. 15. In this arrangement the angle of deflection is transformed into an intensity variation of the light in the image of the object on the photographic plate or screen. The areas of high gradients are indicated by darker or lighter regions in the image. In the Schlieren–Toepler system, two images are produced, one at point "S" of the source and the other at "O" of the object. The knife edge K2 intercepts the image of the source sharpened by knife edge K1. The deflection of the beam produced by a gradient directed upwards will cause the light to miss the K2 edge. If no gradient is present, or its orientation is downwards, then the appropriate light will be blocked. Therefore, the net effect will be that the lighter areas in the image of the object indicate regions in which gradients are directed upwards. The rest of the image will be dark.

The magnitude and direction of the gradient can be studied by moving the knife edge deeper into the image of the light source. Starting from the non-intercepting position, the areas of the object with highest gradients directed downwards will be darkened first, followed by areas with no gradient and then finally areas with gradients directed upwards. Scanning the knife edge allows only analysis of the gradients directed perpendicular to the edge. Analysis in both directions simultaneously can be accomplished by using a centrosymmetric aperture made, for example, of shaded or coloured centrosymmetric rings [19]. The magnitude of the gradient is indicated by darkness or the colour of the image. The direction of the deflection can be determined using an aperture made up of coloured regions [19]. The information about the system can be stored using a holograph set-up which allows careful, time unlimited investigations of the experimental data. The hologram "freezes" the instantaneous information about the gradient field [28].

A very interesting modification of the Schlieren–Toepler system is the Philpot–Svensson method which was used as a detector in moving boundary gel electrophoresis and for centrifuges [17]. The vertical deflection of the light due to the concentration gradient in the electrophoretic cell is transferred into horizontal displacement by the slit which is at an angle to the symmetry plane of the system.
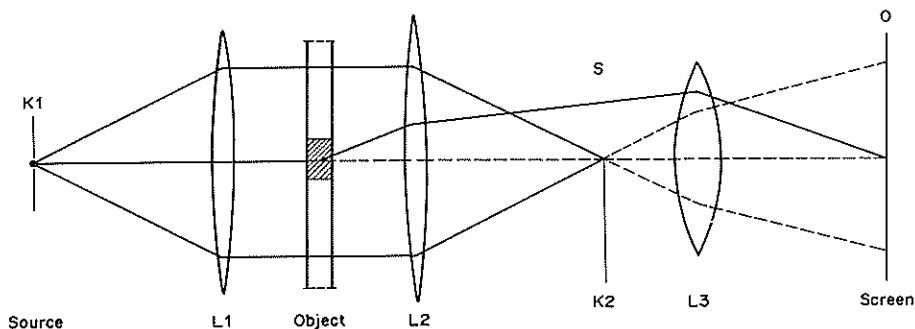

Fig. 15. Example of Toepler Schlieren optical system. L1—Collimated lens; L2—Schlieren head; L3—objective lens; K1—first knife edge (aperture); K2—second knife edge.

Focusing of the slit in the horizontal direction and the cell in the vertical direction using a cylindrical lens generates an image which represents the gradient of refractive index versus the cell dimension. In the more recent version of this system the slit is replaced by a thin wire to improve the precision of the measurement and a phase plate is added to reduce diffraction effects. The diffraction effects are particularly important when highly coherent light sources such as lasers are used to probe the gradients [29].

Another approach used to visualize concentration gradients are the Scale and the Moiré techniques [15, 16, 18, 30]. The Scale method is based on visualization of the refractive index gradients by distortion of a regular pattern when viewing the object [30] (Fig. 16). Information about the refractive index gradient field in the object can be obtained by plotting the shift of every line versus the original position. The displacement of lines is the most pronounced in the areas where the highest gradients of the refractive index are located. The second derivative of the gradient is measured as the distance between lines at the detector plane. In the Moiré method the collimated beam passes through the tested object and then through a set of identical gratings separated by distance Δ. A Moiré pattern is produced by the overlap of the shadows of the first grating with the second grating which is projected on the screen. The observed pattern is affected by the angle at which the light enters the first grating and it therefore corresponds to refractive index gradients present in the object.

It is clear from Eqn (13) that Schlieren optics is a universal method. Any concentration gradient produced by an analyte with a refractive index different from the medium will form refractive index gradients. This property is very useful in chromatographic applications since good separation between components of a sample can be obtained on the column prior to detection. However, in many cases, a situation arises in which more than one concentration gradient is present within the same detection volume. A typical example is the electrochemical interface, where opposing concentration gradients associated with reactants and products are present above the electrode. It should be emphasized that Schlieren optics techniques measure the concentration gradient indirectly and therefore any other parameters which affect the refractive index will interfere with experiment. When present, temperature gradients $\dfrac{dn}{dx} = \dfrac{dn}{dT}\dfrac{dT}{dx}$, or pressure gradients, $\dfrac{dn}{dx} = \dfrac{dn}{dp}\dfrac{dp}{dx}$, will modify the total refractive index gradient signal. In some applications, it might therefore be necessary to be able to monitor selectively one of the species forming the gradient in order to allow a more comprehensive use of Schlieren optics in analytical and dynamic measurements.

5. SPECTROSCOPIC SELECTIVITY

One means of introducing selectivity to the Schlieren optics systems measuring the concentration gradient of a specific species, is to take advantage of the great enhancement of the refractive index close to the resonance frequency of an absorbing species [12, 15, 16]. This phenomenon is produced as the result of significant changes
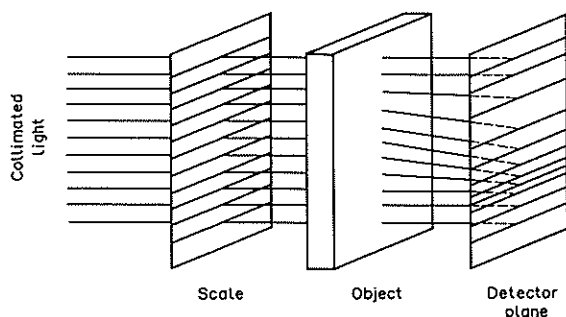

Fig. 16. The Scale imaging method.

in the charge configuration associated with electronic transitions. These changes will induce polarizability and therefore increase the refractivity of the absorbing species. The enhancement factor can be described as the ratio between the refractivity of the species near the resonance wavelength λ_r to that at a wavelength much different from the resonance wavelength, i.e.,

$$\frac{(n-1)_{\text{Small} \,|\lambda-\lambda_r|}}{(n-1)_{\text{Large} \,|\lambda-\lambda_r|}} = \frac{\lambda}{\lambda-\lambda_r}. \tag{22}$$

The relationship between the light wavelength and the refractive index in the vicinity of a Lorentzian absorption band (Fig. 17B) is illustrated graphically in Fig. 17A. As the frequency decreases (wavelength increases) the refractive index first falls to a minimum, then increases through n_0 at the resonance frequency to a maximum and finally levels off to the initial value n_0. Strictly speaking the relationship described by Eqn (22) is valid for gases but similar enhancement is also observed in liquid media.

It is possible to increase sensitivity by over two orders of magnitude and introduce selectivity in Schlieren methods by employing this phenomenon [31]. In this approach, a highly monochromatic probe light beam should be used, with the wavelength close to the value of λ_r for the species of interest, and for which the corresponding refractivity is close to optimum. Therefore, the deflection signal associated with the concentration gradient of an absorbing species will be relatively high when compared to other sources of refractive index gradient such as the presence of another solute in the detection volume, or by pressure or temperature gradients. This technique, however, requires the use of expensive, tunable laser light sources and is limited to those species which adsorb in the wavelength range for which lasers and detectors are available. An additional complication arises because information on other high gradients (temperature, other species, etc.) will also contribute to the overall refractive index gradient.

Recently, another, more general, selective method based on a photothermal process has been introduced [32]. The principle of this approach is illustrated in Fig. 18. The example illustrated is the simple case of a single dimension, constant magnitude concentration gradient. The excitation radiation uniformly irradiates the detection volume in which the chosen absorbing solute forms the concentration gradient. For optically thin samples ($\epsilon \cdot C \cdot L$ is small) and a short excitation pulse (compared to the time for relaxation of the excited state), of intensity I_0 (J/cm^2 per pulse), the amount of energy $\Delta I(x)$ absorbed in the volume will be proportional to the concentration $C(x)$ of the absorbing species:
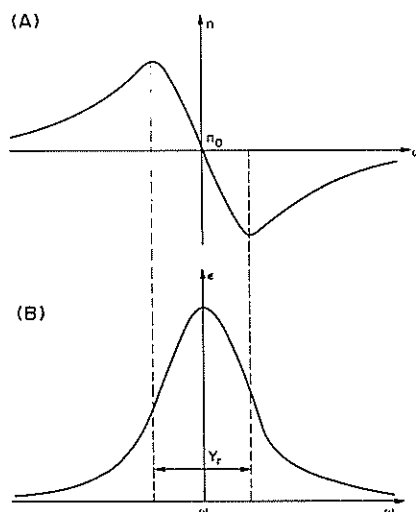

Fig. 17. Refractive index n and absorption coefficient ϵ around a resonant frequency ω_r for a Lorentzian oscillator. Half-width of the absorption curve is y_r.
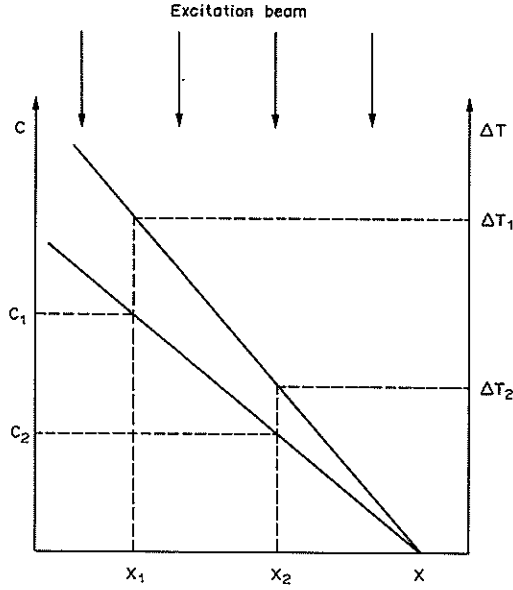
Excitation beam

Fig. 18. Principle of the selective concentration gradient method.

$$\Delta I(x) = 2.303 \, I_0 \, \epsilon_\lambda C(x) \qquad (23)$$

where ϵ_λ is the molar absorption coefficient of the species of interest at wavelength λ [32]. A fraction Z of the absorbed energy will relax into the medium in the form of heat $Q(x)$ (translation motion within detection volume):

$$Q(x) = Z\Delta I(x) = 2.303 \, ZI_0 \, \epsilon_\lambda C(x) \qquad (24)$$

and, in effect, this energy will raise the temperature of the medium. Immediately after the rapid relaxation process, a temperature profile $T(x)$ which corresponds closely to the concentration distribution of absorbing species will be formed:

$$T(x,t{=}0) = \frac{Q(x)}{C_p \rho} = 2.303 \, Z \frac{I_0 \epsilon_\lambda}{C_p \rho} \, C(x,t{=}0) \qquad (25)$$

where C_p is the specific heat at constant pressure of the medium in J/(g·deg), ρ is the density of the medium in g/cm^3, and $T(x)$ is the temperature rise above the ambient condition. Therefore, the temperature gradient at a given position x_0, $\left(\dfrac{dT}{dx}\right)_{x_0}$, density gradient $\left(\dfrac{d\rho}{dx}\right)_{x_0}$ and associated refractive index gradient $\left(\dfrac{dn}{dx}\right)_{x_0}$, formed just after the excitation pulse, will be proportional to the concentration gradient of the absorbing species at the same position x_0 (see Fig. 20B):

$$\left(\frac{dn}{dx}\right)_{x_0} = \frac{dn}{dT}\left(\frac{dT}{dx}\right)_{x_0} = \frac{dn}{dT}\frac{2.303 \, Z\epsilon_\lambda I_0}{C_p \rho}\left(\frac{dC}{dx}\right)_{x_0}. \qquad (26)$$

This refractive index gradient can be measured in the usual way by using the probing beam. The variation of the deflection signal with time describes the thermal relaxation process and carries selective information about the system. The shape and magnitude of this transient signal can be calculated for a model describing the distribution of absorbing species under specified experimental conditions, such as location of the probe beam and excitation pulse length. This can be achieved by solving the differential

equation describing the unsteady heat conduction problem with a heat source [33] where D_T is thermal diffusivity of the medium and

$$\frac{\partial T(x,t)}{\partial t} = D_T \frac{\partial^2 T(x,t)}{\partial x^2} + \frac{1}{\rho C_p} Q(x,t). \tag{27}$$

$Q(x,t)$ is a function that describes the heat generation through the photo-thermal process discussed in detail above (Eqn (24)). The exact solution is always available, and can be found in closed form for some simple cases such as the Gaussian-shaped concentration profiles associated with injection plugs in flow injection analysis and the solute peaks in chromatography [34]. In more complex cases, the heat diffusion process can be analysed numerically [35], or by Fourier Transform methods [36].

To solve the above differential equation with these techniques we first assume a short excitation pulse. Under such conditions, the heat transfer problem can be simplified to an unsteady state, one-dimensional heat conduction problem,

$$\frac{\partial T(x,t)}{\partial t} = D_T \frac{\partial^2 T(x,t)}{\partial x^2} \tag{28}$$

with the initial temperature distribution $T(x,0)$ described by the photo-thermal process (Eqn (25)). Response of the system to an excitation period of a given length can be found by convoluting it with the solution to the differential equation which describes the impulse response function. Equation (28) can be solved by numerical methods frequently used by engineers [35]. However, if homogeneous heat diffusivity is assumed throughout the system, then the solution to the problem can be obtained more readily using Fourier transform methods. The Fourier transform of the solution to the differential Eqn (28) is found to be [33]:

$$FT[T(x,t)] = \exp[-D_T\omega^2 t] \, FT[T(x,0)]. \tag{29}$$

In other words, the solution to the unsteady state heat transfer problem with an initial temperature distribution $T(x,0)$, can be found essentially by applying a filter to the initial temperature distribution $T(x,0)$, of a frequency response given by: $\exp[-D_T\omega^2 t]$. This filter describes thermal relaxation processes. These calculations can very readily be handled by a Fast Fourier transform subroutine. Direct comparison between the experimental data and the model is possible: this enables a confirmation of the postulates regarding the spatial distribution of the absorbing species.

On the basis of theoretical and experimental investigations, some important conclusions about the capabilities of Schlieren optics methods can be drawn. For example, it is expected that the spatial resolution Δx of the selective concentration gradient method associated with Schlieren optics will depend on the length of time Δt after the beginning of the pulse during which the signal is collected [34]

$$\Delta x = \frac{4\Delta t k^{1/2}}{\rho C_p}, \tag{30}$$

where k is the thermal conductivity. This relationship clearly indicates that, in order to obtain an accurate representation of the concentration distribution as a temperature profile, short excitation pulses should be followed by immediate measurement. For example, to achieve spatial resolution of 1 μm in liquid media, the signal should be collected within 10 μs after a short excitation pulse. It should be emphasized that independently of how short the pulses are, Δt cannot be smaller than the relaxation time of the excited-state species.

Equation (26) indicates that the sensitivity of the selective concentration gradient method is dependent on the medium, and is proportional to $\dfrac{dn}{dT}\dfrac{1}{\rho C_p}$ [34, 37] for a short

excitation pulse. If a chopped excitation beam is used, the sensitivity will then be proportional to $\dfrac{dn}{dT}\dfrac{1}{k}$ [34, 38]. The concentration gradient method has a number of unique properties compared to other photothermal schemes. For example, it does not require a highly focused beam, but rather excitation radiation which uniformly irradiates the detection volume. Therefore, broadband light sources associated with FT techniques can be used [20]. This will allow the collection of a whole spectrum of absorbing species forming the gradient. In addition, less manageable (focusing properties) but more selective regions of electromagnetic radiation, such as microwaves, can be explored [34]. It should be mentioned that photothermal processes produced by microwaves (cooking ovens), have already been applied commercially for some time.

The selective Schlieren optics method is related to other probe/pump two beam photothermal techniques [39] (Fig. 19). However, there are very important differences between the concentration gradient method and other photothermal schemes which affect the optimum experimental conditions and the scope of their applications. In thermal lensing [40, 41, 42], photothermal deflections [21, 43] or cross beam photothermal refraction [44, 45] (Fig. 20A), the refractive-index profile corresponds to the excitation beam intensity profile. Therefore, the signal in these techniques is proportional to $\left(\dfrac{dI}{dx}\right)_{x_0} C(x_0)$ while in the concentration gradient method (Fig. 19c), it corresponds to $I(x_0)\left(\dfrac{dC}{dx}\right)_{x_0}$. Surface photothermal deflection (21, 46, 47) measures the concentration of the species on the surface. The signal in this method is related to the temperature gradient created above the surface after heat has been allowed to diffuse from the surface to the portion of the medium through which the probing beam propagates
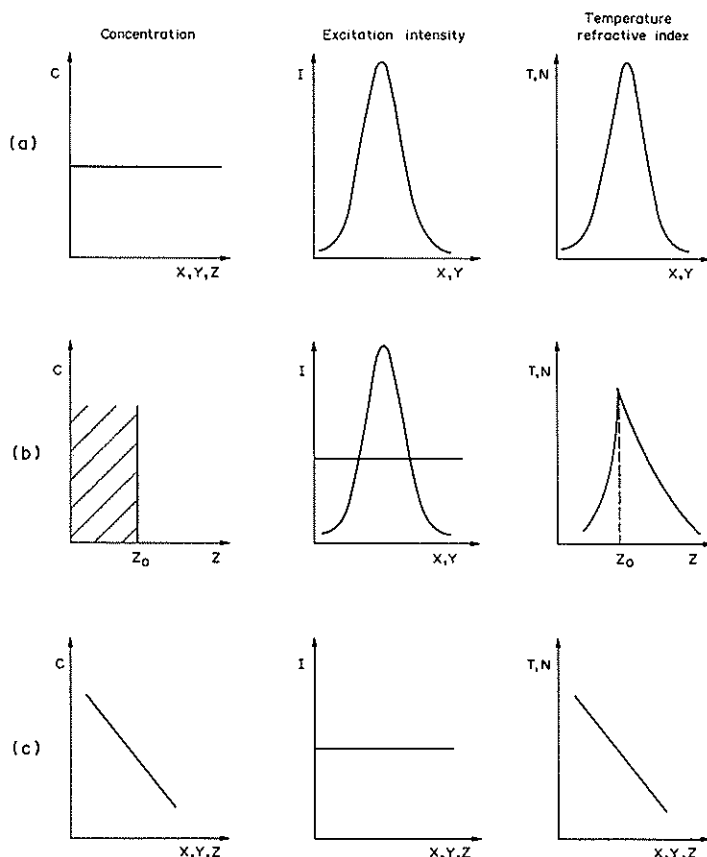

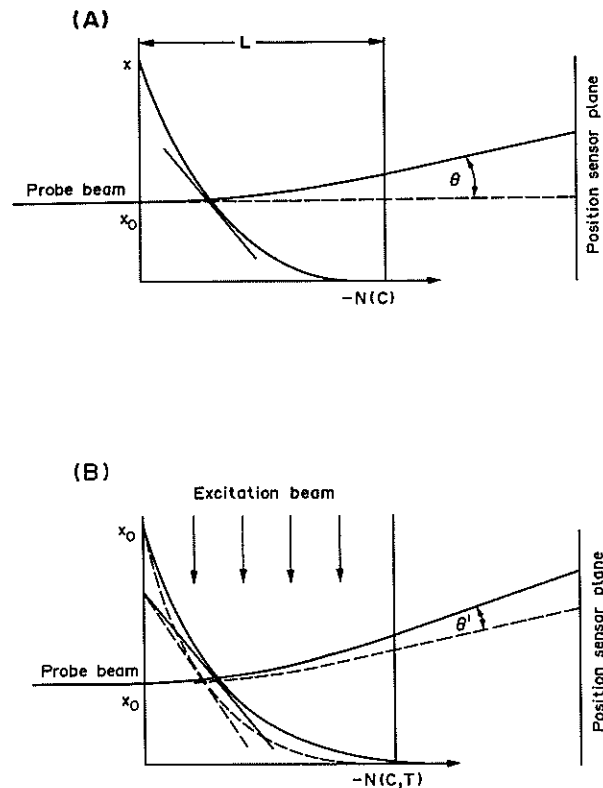Fig. 19. Probe/pump two beam photothermal schemes. Adapted with permission from Ref. [36].

Fig. 20. Schematic of the concentration gradient method: (A) universal mode; (B) selective
mode. Adapted with permission from Ref. [36].

(Fig. 19b). The general concept of the deflection method described above is summarized
in Fig. 20, illustrating the simplest one-dimensional scheme. A probe beam passes
through the detection volume at x_0, and its signal is proportional to the gradient along

its path. There it encounters the concentration gradient $\left(\dfrac{dC}{dx}\right)_{x_0}$ and undergoes deflection

by $\theta = \dfrac{L}{n}\dfrac{dn}{dC}\left(\dfrac{dC}{dx}\right)_{x_0}$ (31) (Fig. 20a). After introduction of the excitation pulse of

intensity I_0, it experiences an additional deflection of magnitude

$$\theta' = \frac{L}{n}\frac{dn}{dT} 2.303\, Z\, \frac{\epsilon_\lambda I_0}{C_p \rho}\left(\frac{dC}{dx}\right)_{x_0} \tag{32}$$

immediately after the relaxation process (Fig. 20B). The selective signal associated
with θ' can be generated only by an absorbing species. For example, if there are a
number of various concentration gradients in the detector volume, all of them will
contribute to θ but θ' will only correspond to the gradient which absorbs the excitation
energy.

The usual configuration of the signal processing system associated with the
concentration gradient method is shown in Fig. 21. The silicon sensor collects
information about the change in position of the probe beam. In liquid and solid media,
the mass diffusivities of the species of interest are much smaller by comparison with
the thermal diffusivities of these media. Therefore, the universal information associated
with the direct measurement of the concentration gradient distribution is included in
a slowly varying component of the signal. The high frequency deflection signal θ'
contains selective information related to the fast-decaying temperature gradients
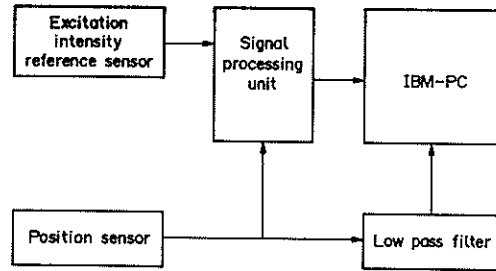generated during the experiment. This component of the signal is analysed by a

Fig. 21. Experimental arrangement associated with the concentration gradient method. Adapted with permission from Ref. [34].

processing unit. For chopped excitation energy sources, lock-in detection should be applied. For pulsed sources, gated detection should be used. The selective signal is compensated for energy fluctuations in the excitation source with the help of the reference sensor. Both signals (universal and selective) are then stored in a computer for further analysis.

Figure 22 summarizes the analysis procedure for a Gaussian solute plug present in a flowing stream. The universal mode of Schlieren optics detection produces a trace which corresponds to the derivative of the concentration profile (Fig. 22A). If the solute absorbs excitation energy, the high-frequency periodic deflection signal associated with the selective mode of detection will overlap the slowly varying derivative trace (Fig. 22B). Figure 22C represents a periodic signal separated from the universal trace. It is clear that the amplitude of modulation is proportional to the gradient (slope of the Gaussian concentration profile). Finally, after the signal processing unit, the magnitude of the selective signal versus time is obtained (Fig. 22D). As expected, it corresponds to the universal trace, since the same solute is detected by the two different methods.
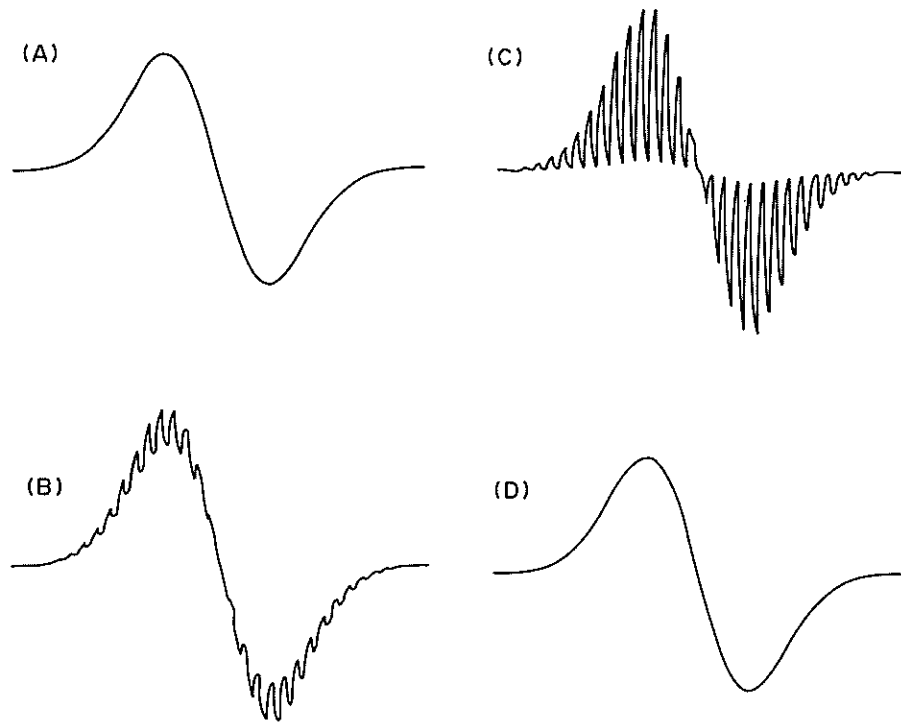
Fig. 22. Illustration of the concentration gradient method used to detect Gaussian peak. (A) Universal information only; (B) selective and universal information combined; (C) selective information only; (D) selective information after signal processing unit. Adapted with permission from Ref. [34].

6. ANALYTICAL APPLICATIONS

The deflection of the probing beam is proportional to the concentration gradient over four orders of magnitude of concentration. In the universal and selective modes of the operation, the detection limits are close to 10^{-2} M/m [25] and 10^{-4} M/m [34], respectively, for a 0.1 mm diameter detection cell, a small molecular weight solute and a moderate value molar absorption coefficient. These limits are still high compared to theoretical predictions (about 10^{-3} M/m and 10^{-8} M/m), especially for the selective mode of operation. They can be substantially improved by reducing background absorption, combining concentration gradient with non-uniform excitation in the same experiment (Fig. 19), improving signal analysis methods and using multiple-pass techniques [48]. The simple optical arrangement of the system with a laser diode as a source of probe beam allows the design of robust and inexpensive analytical sensors. To date, only a limited number of applications have been explored experimentally for this high sensitivity, single dimension system. The results are very promising and they are summarized below, together with a discussion of even more interesting future applications of this method. The focus of the discussion is placed on principles and concepts behind the optimum design of highly sensitive detectors devices for various analytical techniques. Further details about the particular applications can be found in the appropriate references.

6.1. *Detection in flow injection analysis*

Design of the detector is very important in concentration gradient methods. The signal in this technique is proportional to the gradient, and therefore the sample must be introduced so as to form the highest possible change in concentration in the detection region. Figure 23 shows the cell design which has been used for this purpose. The analyte is introduced into the cell with the help of a small diameter (ID ~50 μm) fused silica capillary which has been sharpened at its tip to improve the hydrodynamic flow pattern around the capillary. This capillary is inserted into the centre of a detector cell consisting of a square piece of glass tubing. As Eqn (13) indicates, the sensitivity of the deflection method is proportional to the cell dimensions as well as concentration gradients generated in it. Therefore, the largest cell diameter still consistent with good
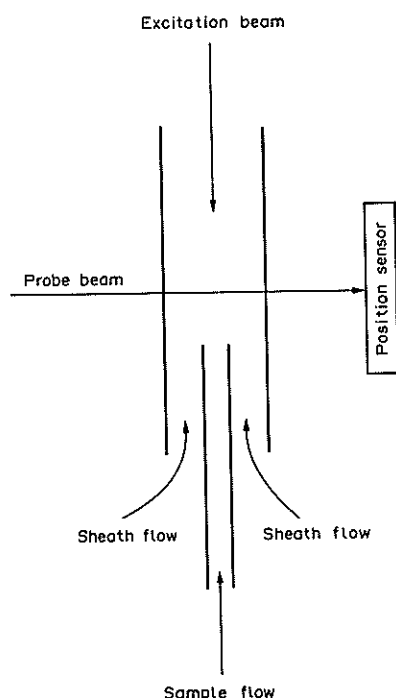

Fig. 23. Schematic of the concentration gradient detector for flowing samples. Adapted with permission from Ref. [34].

hydrodynamic behaviour and which will not broaden the plugs significantly during flow should be used. This diameter can be as large as 1 mm [23]. However, as the diameter increases, more analyte needs to be injected to produce similar sensitivity. The probe beam propagates through the cell above the tip of the capillary. The analyte is introduced into the detection volume in the form of small plugs. Then the auxilliary flow (marked as "sheath flow" on Fig. 23) of the pure solvent flowing around the capillary pushes the analyte into the probe beam region.

This process of plug formation was carefully studied using a magnifying lens and a dye as a solute. Figure 24 shows sample flow through the system. During slow introduction of solute into stationary fluid, the sample forms a thick disk located over the tip of the capillary (Fig. 24A). The solvent flow then pushes the solute through the probe beam. At the same time the flow profile extends the analyte in a vertical direction (Fig. 24B, C).

Figure 25 shows an example of a flow injection experiment, consisting of a series of injections of solute solution. The first part of the derivative is higher and narrower than the second part. This result can be explained by the observed flow pattern and is illustrated in Fig. 24. The process generates a pear-like solute profile with broad high gradients in front with a more gradual change to a thin tail.

The Schlieren optics method is capable of monitoring a single component present in the injected mixture. This can be done using the selective mode of concentration gradient method described above. The excitation beam is introduced with the help of an optical fiber inserted into the detector volume from the far end of the square tube. In this scheme, the thermal relaxation transient is measured following the excitation pulse [34]. The concentration gradient method provides both universal and spectroscopic
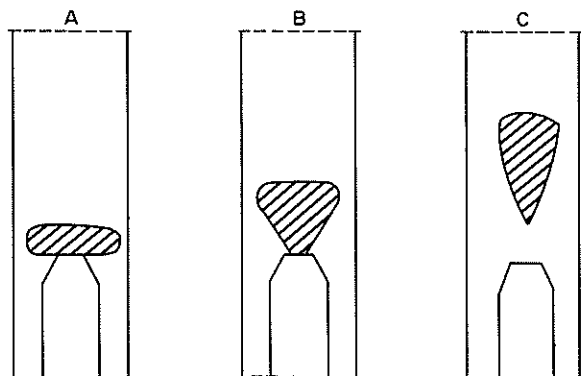

Fig. 24. Flow profiles of sample injected to the detector cell from Fig. 23.
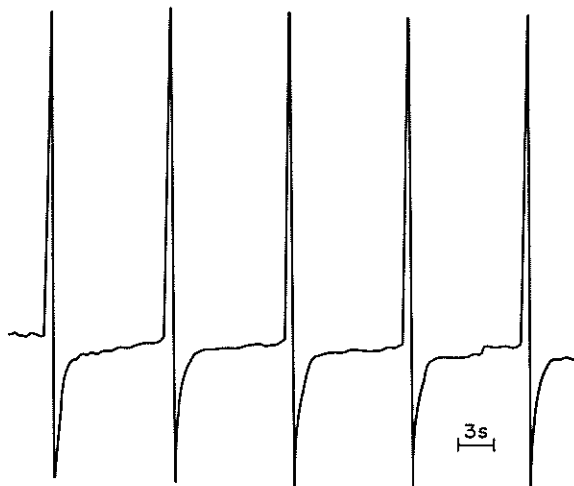

Fig. 25. Series of 8 nl of 10^{-4} M sucrose solution injections into detector cell from Fig. 23. Solvent flow rate, 0.4 μl/min. Adapted with permission from Ref. [23].

information at the same time. Therefore, an estimation of important parameters such as the extinction coefficient for a given pure solute in a sample mixture can be done. This information is often used to determine purity, biological activity and freshness of samples [34]. The absorption properties of the analyte can be measured simultaneously at several wavelengths by modulating each excitation beam at various frequencies and then selectively detecting each frequency component.

The flow injection method described above can be used to continuously monitor the composition of a mixture such as effluents from a liquid chromatography column [23]. The detection can be performed directly if the eluting peaks produce large gradients. This application of the method is discussed in the following section.

The detection limit for the Schlieren optics method in flow injection analysis should be described in refractive index gradient units. However, for a given experiment and solute, it can be presented in concentration units. The detection limit $(3 \times$ RMS noise) for a 200 μm ID detector is about 5×10^{-6} M of sucrose injected for a single probing beam and 7×10^{-7} M for the differential arrangements discussed previously (Fig. 12E). This corresponds to 3×10^{-8} refractive index units difference between analyte mixture and pure solvent [25]. Considering the small detection volume ($\sim$4nl) the total amount of sample injected at the limit is in the subpicogram range. In the selective mode of detection, the limits are two orders of magnitude smaller when compared with the universal method, which allows sub-femtogram detection of strongly adsorbing dyes such as Congo Red [34].

6.2. Detector for ultra high efficiency capillary separation methods

The low detection volume, high sensitivity, derivative response and universal nature of the concentration gradient method makes it very attractive for application to high efficiency capillary methods such as capillary electrophoretic methods and capillary liquid chromatography [49, 50]. The high efficiency associated with these methods (reaching a million theoretical plates) ensures good separation between the sample components. Therefore, the most appropriate instrument for this application is the universal detector, since it will enable monitoring of components present in the sample mixture. Broadening of the injection plug during transport through the open tubular capillary is much smaller than that found for packed chromatographic columns and hence much sharper bands are produced at the detector. However, significant dispersion of the injection plug occurs with time. Thus, the concentration gradient detector is most effective in short-column, rapid separations. Figure 26 shows a one minute electrophoretic separation using a 2 cm capillary [51]. In this experiment, the analyte
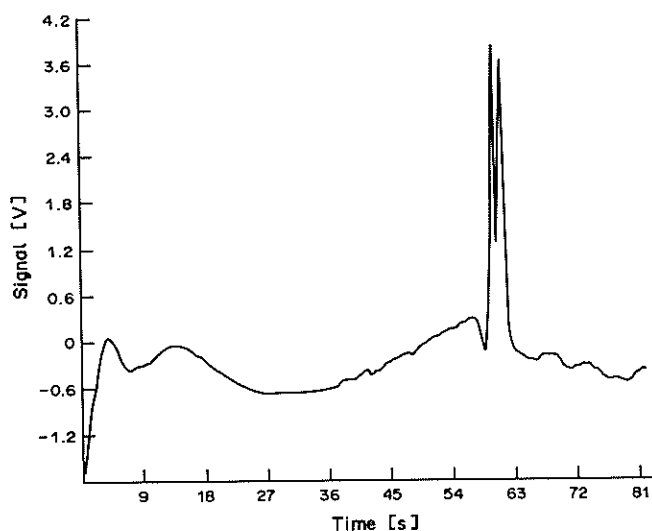

Fig. 26. Rapid capillary moving boundary electrophoretic separation of urea from sucrose. 2 cm of 50 μm ID capillary, pH 3 buffer. 10^{-4} M concentration of each analyte.

was detected by focusing the light beam directly into the capillary. This method allows rapid analysis of simple mixtures. However, because the capillary is short, the separation between analytes in many cases might not be sufficient. In order to ensure high-sensitivity detection in the long-column separation, the broader bands eluting from the narrow bore capillary can be expanded to a larger diameter cell (Fig. 27). After this has been done, the sensitivity of the detection will increase by $(d_2/d_1)^3$ where d_1 is the capillary column diameter and d_2 the diameter of the cell: the $(d_2/d_1)^2$ improvement is due to the reduction in the width of the band and at the final (d_2/d_1) is due to the increase of the probe beam pathlength [23].

In the discussion above, we assumed that no mixing and no diffusion occurred during the expansion process. Mixing can be minimized by using a cone shaped detector or by applying sheath flow. The design of the detector cell in the second case is similar to that shown in Fig. 23. The small auxilliary flow of solvent is continuous during the separation process and constitutes sheath flow, which cushions the expansion process and prevents mixing. However, it is impossible to eliminate diffusion, and therefore sharpening of the bands by expansion of the effluents is only partially effective. This process should be optimized for each type of separation in order not to limit resolution.

The derivative nature of concentration gradient detection allows effective removal of the refractive index drifts produced by temperature fluctuation or composition changes of the mobile phase, for example in the solvent programming often used in HPLC [23]. Figure 28 summarizes the properties of a gradient detector applied to monitor the effluents in the capillary electrophoretic separation of underivatized amino acids. In this experiment, both capillary and sheath flows are generated using electro-osmotic flow [25] (Fig. 29). The three derivatives are clearly observed and no drifts are detected in the baseline (Fig. 28B). Figure 28D shows the integral of the above separation, which corresponds to the electropherogram monitored by the refractive index method. Now peaks are present rather than derivatives. These signals are not as well resolved as in the previous case. Also, the drift in baseline is clearly visible, indicating the presence of temperature fluctuations. The drifts in the baseline can be significantly reduced if the regions of peaks are the only sections integrated rather than the full electropherograms.

A direct way of generating peaks with the gradient detector rather than calculating the derivatives is to apply moving boundary electrophoresis rather than the zone technique. In this frontal mode of operation, the sample is introduced as a front rather than the usual plug. The separation in this system will produce a series of concentration steps associated with given solutes (Fig. 3D), which will be detected as peaks by the derivative detector (Fig. 3C). This scheme has several important advantages when
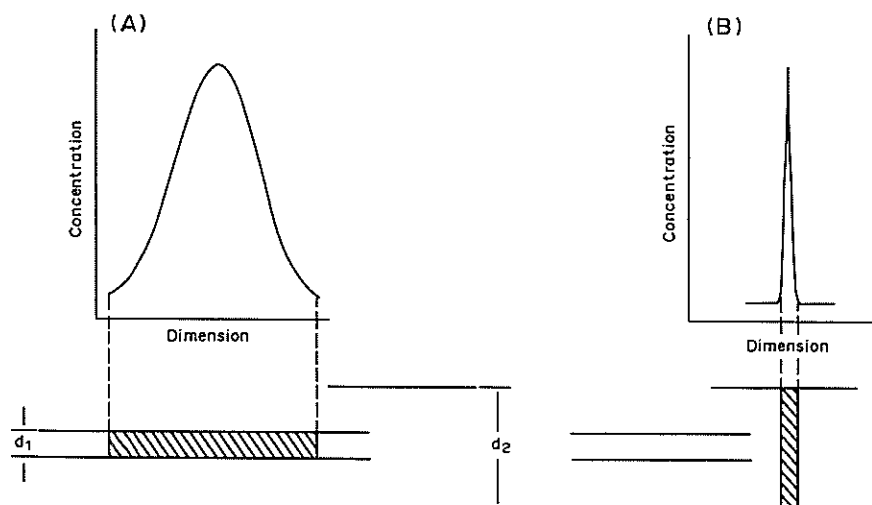

Fig. 27. Sensitivity enhancement in the effluent expansion method. (A) Broad Gaussian in capillary; (B) narrow Gaussian in larger detector cell.
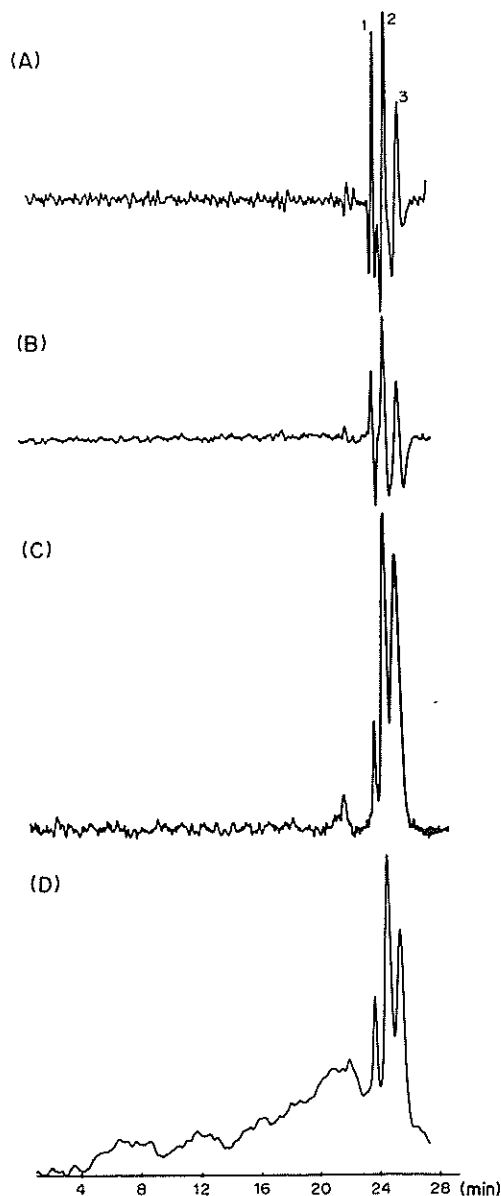
Fig. 28. Capillary electropherograms of three underivatized amino acid mixture (about 2 μm for all); Glycine (1), L-Alanine (2), L-Asparagine (3); 0.1 M phosphate buffer, pH7; voltage 10 kV. (A) Sequential differential concentration gradient detection of zone injection; (B) concentration gradient detection of zone injection; (C) concentration gradient detection of frontal injection (moving boundary electrophoresis); (D) integral of signal from Fig. 27.

compared with zone electrophoresis. It is much easier to produce a sharp front than a sharp and narrow plug and this type of injection does not discriminate as does plug injection. A significant improvement in sensitivity can be made, since the maximum concentration of the sample is not diluted during the separation process. In this method, separation is not affected by peak tailing since only the fronts of peaks are detected. Figure 28c shows a moving boundary electropherogram of the same mixture [50]. The increased sensitivity is clearly visible. Figure 26 also shows moving boundary separation. Similar advantages can be obtained when using frontal chromatography.

Figure 27a shows the application of the differential concentration gradient detection scheme described previously (Fig. 12E) to the detection of the same sample mixture [25]. Now, the separation between signals is significantly enhanced, as compared with concentration detection (Fig. 28D), because of the narrow derivatives.
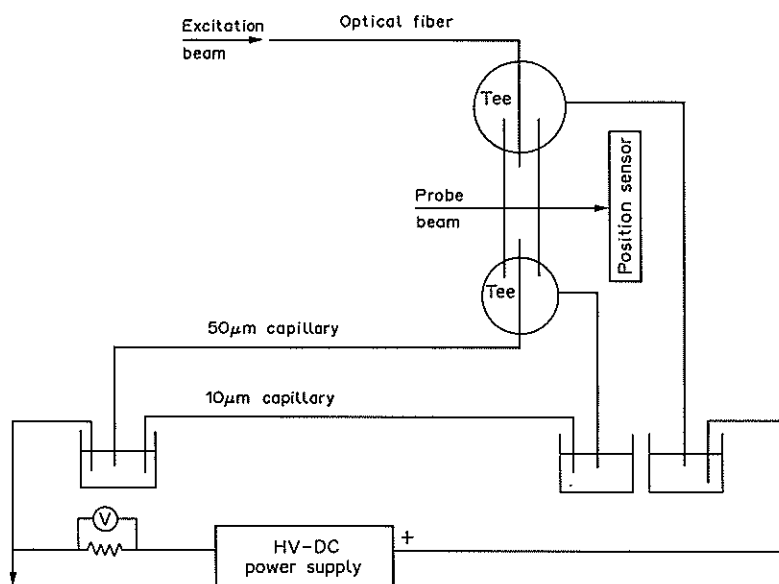
Fig. 29. Schematic of capillary zone electrophoresis experimental arrangement. Sheath and capillary flows are generated using electro-osmotic force. Adapted with permission from Ref. [25].

Differential detectors can be used effectively to study the shapes of eluting bands on the basis of their injection profiles. This approach is used for studying the kinetics and thermodynamics of chemical interactions during the separation process.

Introduction of the excitation beam to the detection volume enables simultaneous, selective, spectroscopic detection. This method can be used to allow identification of separated peaks [49]. The other potentially important area of application of the selective gradient method is the indirect absorption technique. Due to its differential nature, this method can effectively eliminate drifts associated with high background absorption which will significantly improve the dynamic reserve of the technique.

6.3. Detector for capillary isotachophoresis

In isotachophoresis ionic analytes are separated into pure distinct zones arranged into a stacked fashion according to their mobility and migrating with constant velocity towards the common electrode (Fig. 30a). In this technique the sample is introduced between leading and tailing electrolytes which have higher and lower mobility, respectively, than the components of the analytical mixture. The boundary between zones formed in this technique is very narrow due to the sharpening effect and the concentrations of analytes and are high in their zones because of the concentration effect [52–54]. These properties of the method ensure the formation of high concentration gradients at the zone boundaries which can be readily detected by the gradient method (Fig. 30b). The high spatial resolution and universal response of the gradient detector allows sensitive and quantitative detection of all zones produced during isotachophoretic separation [55]. The above short description clearly indicates a good match between both methods. A more detailed discussion and some examples are listed below to better illustrate the above points.

The boundary sharpening effect of isotachophoresis has a unique capability to eliminate the effect of diffusion on zone broadening. This is caused by the different electric field strengths which exist in various zones according to analyte mobilities. The sample component which is not native to a given zone is accelerated or decelerated and therefore expelled from it. The net result is that a sharp boundary is maintained between the zones throughout the separation process. The boundary width Δx can be estimated from the equation [53]:
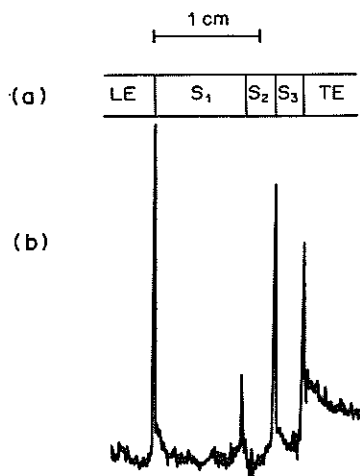
Fig. 30. Capillary isotachophoretic separation of low molecular weight carboxylic acid mixture (S_1, S_2, S_3). Leading Electrolyte (LE)-Chloride ion; tailing electrolyte (TE)-MES.

$$\Delta x = \frac{4RT}{FV}\frac{u}{\Delta u} \tag{33}$$

where R is the universal gas constant, T is the temperature in K, F is the Faraday constant, V is the average field gradient in the capillary, u is average mobility of analytes forming boundary and Δu is the difference in their mobilities. It can be calculated that in most of the cases the boundary is expected to be only several tens of microns wide and can be sharpened by increasing the voltage. This results in higher sensitivity of the gradient detector, which is illustrated in Fig. 31. A three-fold increase in the electrical field doubles the magnitude of the signal.

There is always concern about being able to detect the trace components of the sample. The concentrating effect of isotachophoresis eliminates this problem. This effect is described by the so-called "regulating function" [54]. It states that the ionic concentration in a separated sample zone will adapt itself to the concentration of the preceeding zone by the following relationship:

$$\frac{C_A}{C_A} = \frac{u_A(u_R + u_B)}{(u_A + u_R)\,u_B} \tag{34}$$

where u is the ionic mobilities of the sample component in the appropriate zones A, B, and the counter ion R, and C is the concentration of the species in the appropriate zone. The above relationship indicates that at steady state the concentrations in each zone are similar in magnitude and are independent of the initial concentrations of various components in the sample mixture. However, since the mass balance needs to apply in this system this means that the zone width becomes progressively narrower with decreases in concentration. Therefore, in order to detect trace amounts of analyte it is necessary to use a detection technique which has high spatial resolution. The laser beam can be easily focused to a spot size of a few microns which will allow very narrow zones to be detected. Figure 32 illustrates the detection of sub-millimeter zones. The high spatial resolution of the gradient method will also allow proper quantitation by accurate measurement of the zone lengths. It can be also noted from Figs 30, 31 and 32 that the derivative response of the gradient method is well suited to capillary isotachophoresis as the "step-like" changes in the concentration are converted to peaks. In addition, the universal nature of the method ensures detection of all zones produced in the separation. Similar advantages can be obtained when using this detection method with displacement chromatography.

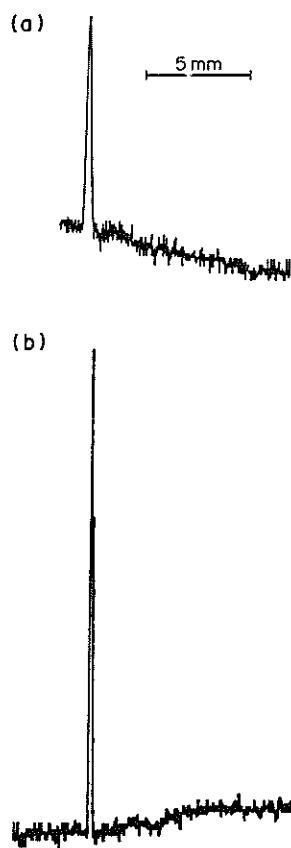There are many applications of isotachophoresis [52, 53, 54]. Its resolving power can

(a)

|___5 mm___|

(b)

Fig. 31. Capillary isotachophoretic boundary between Cl⁻ and MES. Produced at (a) 3kV,
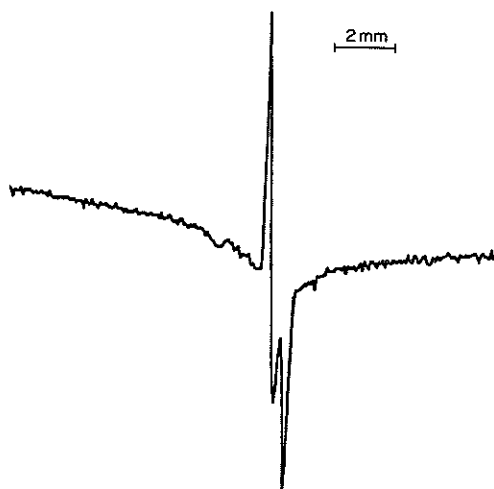(b) 9kV.

|_2mm_|

Fig. 32. Detection of sub-micromole concentrations of citrate and acetate ions by capillary
isotachophoresis with the concentration gradient detector, concentration of Cl⁻ (LE) and MES
(TE) are at 10 micromole level.

be comparable to capillary zone electrophoresis. In addition, capillary isotachophoresis
is more suited for micropreparative work because of the large diameter of the separation
capillary [55]. Isolation of the components into pure zones can be used effectively for
qualitative analysis with different spectroscopic methods including mass spectrometry
[56]. The concentration gradient method can be very helpful in such a scheme by
detecting the arrival of new zones.

6.4. Detector for HPLC

The concentration gradients associated with solutes eluting from typical HPLC columns are small due to significant band broadening during the separation process with the result that sensitivity of the gradient detection in the axial direction is poor [23]. However, after modification of the system, limits of detection can be achieved similar to those of flow injection analysis (23, 57, 58). To accomplish this task the two approaches illustrated in Fig. 33 can be used. In the first method the HPLC column effluent is divided into equivalent portions spaced by plugs of pure mobile phase (Fig. 33a). If the solute is eluting from the column, high concentration gradients are generated at the boundary between the two plugs which can be readily detected. In practice this approach is implemented by using the system designed for flow injection analysis (Fig. 23) and the effluent from a column is delivered as the analyte. In this approach the lock in amplification is very effective in further lowering the limit of detection by narrowing the bandwidth of the measurement [23]. It should be noted that in this approach the high gradients are generated not only along the flow in the axial direction but also closer to the wall in the perpendicular radial direction as well (see Fig. 24). Therefore, if uninterrupted delivery of pure mobile phase in the form of the sheath flow is provided around the effluent, the high gradients will be produced continuously in the perpendicular direction [57]. The latter approach, which measures the gradients in the axial direction, will not require a high speed valve as in the previous method. In practice the additional sheath flow is unnecessary. A similar effect is generated at laminar flow conditions in the detector cell. The velocity of the mobile phase close to the detector wall is low compared to the centre (Fig. 33b). Therefore the composition of the effluent is highly inhomogeneous in the perpendicular direction when a solute plug arrives at the detection volume [57].

The concentration profile $C(x,r)$ expressed as a function of the axial (x) and the perpendicular, radial (r) positions generated by the laminar flow in the tube can be described by the equation derived by Taylor [59]:

$$C(r,x) = C(r=0,x) + \frac{u}{4D_m}\left(r^2 - \frac{r^4}{2R^2}\right)\frac{dC\,(r=0,x)}{dx} \qquad (35)$$

where $C(r=0; x)$ and dC/dx $(r=0,x)$ are the concentration and its gradient, respectively, in the center of the tube expressed as a function of the axial position x; R is the
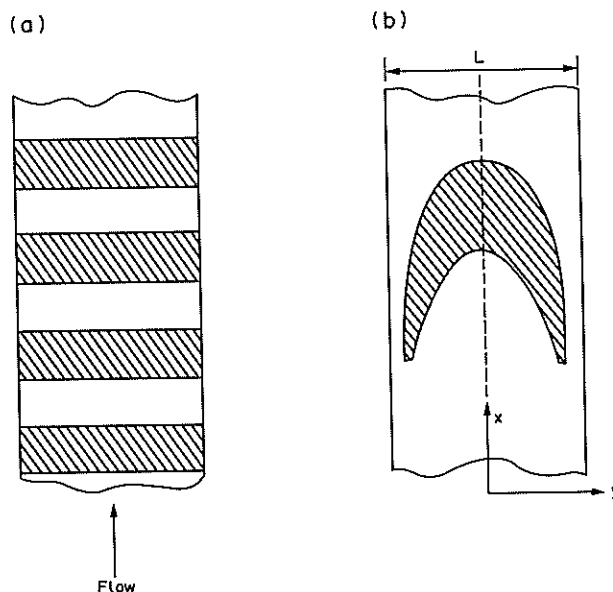

Fig. 33. High sensitivity concentration gradient detection for HPLC effluent: (a) modulation method using FIA system for Fig. 23; (b) sample plug profile produced in parabolic flow indicating high concentration gradient in the direction perpendicular to the flow direction.

diameter of the tube, D_m is the diffusion coefficient of the solute in the mobile phase and u is its linear velocity. The parabolic concentration profile of the solute (Fig. 33b) will produce symmetric "concentration lens" in the detection cell [60]. The optical inhomogeneities associated with the concentration profiles are considered to limit detection in absorbance method and Schlieren methods are very useful in studying these effects [60, 61, 62]. This phenomenon can be used effectively in gradient detection, for example, by probing the curvature of the parabolic lens. Experimentally, a square cell was used (Fig. 33b). The gradients of concentration in the horizontal (y) direction which define the curvature of the refractive index in this experiment, can be calculated as a derivative of $C(x,y)$ from Eqn (35), where the radial position r is replaced with the perpendicular dimension y:

$$\frac{\partial C(y,x)}{\partial y} = \frac{u}{2D_M}\left(y - \frac{4y^3}{L^2}\right)\frac{\partial C(y=0,x)}{\partial x}. \tag{36}$$

The maximum of the curvature can be derived from the condition:

$$\frac{\partial^2 C(y,x)}{\partial y^2} = 0$$

which is reached for $y = L/(2\sqrt{3})$ (about half way between the center and the cell wall). At this position the gradient in the horizontal direction is at the maximum and at all times can be related to the concentration gradient produced at the center of the flow in the vertical direction:

$$\frac{\left(\dfrac{\partial C}{\partial y}\right)_{max}}{\left(\dfrac{\partial C}{\partial x}\right)_{y=0}} = 0.193 \frac{uR}{D_M}. \tag{37}$$

In practice Eqn (37) only approximates this ratio since in the Gaussian profile case the assumption of the constant gradient in flow direction made by Taylor [59] is not valid. For typical experimental arrangements this ratio is about 2000 ($D_M = 10^{-5}$ cm^2/s; $u=1$ cm/s, $L=1$ mm), which clearly indicates that under the laminar flow conditions the concentration gradients are much higher in the horizontal than in the axial direction. This in turn will enhance the sensitivity of concentration gradient detection by several orders of magnitude. In practice the total increase in the gradient magnitude measured in the above method is composed of two factors, one associated with the parabolic flow profile discussed above and the other with the expansion of the effluent as shown in Fig. 27. To obtain the highest sensitivity in this detection scheme the volume of the cell should be optimized carefully. A detector that is very small compared to the peak volume will limit the sensitivity, while a large cell will reduce the resolution. The example discussed above clearly demonstrates that good understanding of experimental details can lead to sensitive gradient detection.

The symmetry of the parabolic flow can be explored to enhance detection by using the dual beam set-up illustrated in Figs 12E and 13 and already discussed previously. The two probe beams are spaced by such a distance around the centre of the flow cell to probe the highest gradient generated in the horizontal direction. An inexpensive detection scheme based on this principle is illustrated on Fig. 34 [57]. It is composed of laser diode, lens, beam splitter, aperture and two photodiodes. The "parabolic lens" generated in the cell during elution of the solute will deflect both beams towards or away from each other depending on the orientation of the refractive index gradient.This will result in an increase or decrease in the intensity of the light reaching the detector located on the other side of the cell [25]. In addition to simplicity, this system rejects the deflection of both beams in the same direction and therefore eliminates mechanical vibrations, laser beam pointing drifts and temperature gradients in the mobile phase
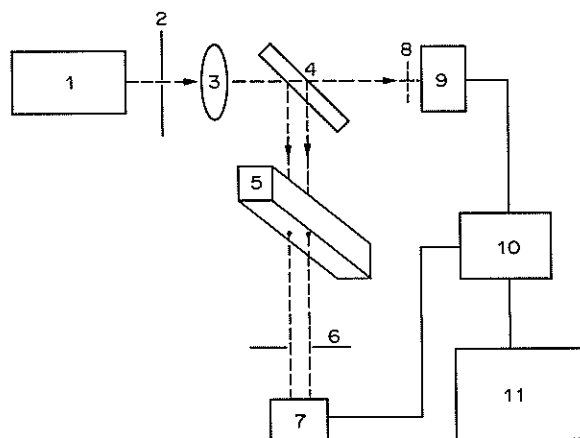
Fig. 34. Schematic representation of dual probe beam experimental setup for HPLC detection. (1) He–Ne laser, (2) iris, (3) lens, (4) beam splitter, (5) square cell, (6) adjustable aperture, (7) photodiode detector, (8) neutral density filter, (9) reference detector, (10) differential amplifier, (11) computer.

[57]. Detection limits obtained using the methods outlined on Fig. 33 are over an order of magnitude lower compared to conventional refractive index detectors. In addition, the cell volume is about 0.1 μl and can be made several orders of magnitude smaller, which makes this detector not only applicable to conventional HPLC but also to microscale liquid chromatography. Figure 35 shows the signal produced by eluting a peak consisting of a few picomoles of polyacrylic acid $\overline{MW} = 250,000$. This also clearly illustrates the high sensitivity of the gradient detector towards high molecular weight compounds due to the large dn/dC, as shown in Eqn (14).

6.5. Spectroelectrochemical sensor

A considerable amount of information regarding the electrode process can be obtained using the simple, single dimension Schlieren optics system illustrated in Fig. 36. A focused probe laser beam propagates close to the working electrode. The excitation laser beam can be introduced from above with the help of an optical fiber [36]. Reference and auxilliary electrodes ensure proper operation of the electrochemical cell.

Initial measurements indicate that the concentration gradient method provides information similar to electrometer detection in cyclic or step voltammetry [63]. The only difference is related to the time delay associated with the diffusion of the
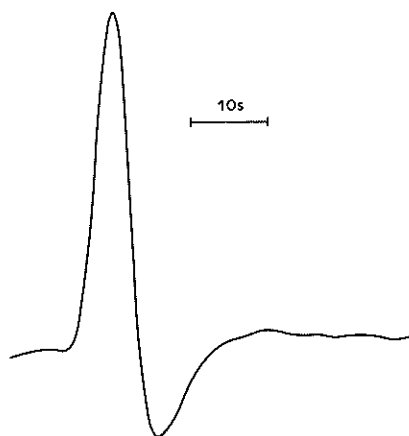
Fig. 35. Signal detected by elution of a few pmol of polyacrylic acid using experimental set-up from Fig. 34.

Excitation beam

Laser — Lens — [chamber] — Position sensor
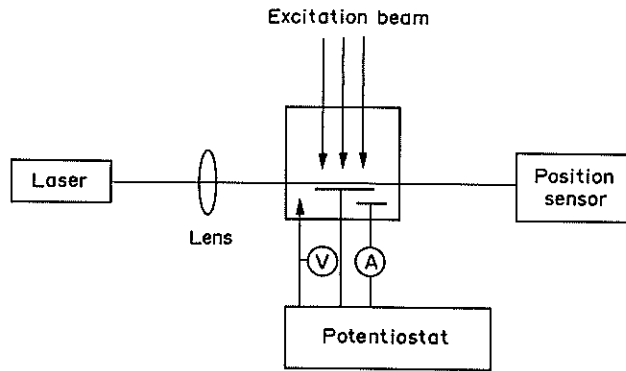
(V) (A)

Potentiostat

Fig. 36. Example of experimental set-up in electrochemical concentration gradient detection.
Adapted with permission from Ref. [36].

electrogenerated species into the probing beam region. This observation should be expected, since the electric current magnitude (number of electrons/time) detected by the electrometer is proportional to the mass flux of reactant that diffused to the electrode surface. This flux, by the Fick's Law relationship

$$M_A/S = -D_A \frac{dC_A}{dx},$$

(38)

where M_A is the mass flux of reactant A, S is the surface area of the electrode and D_A is the corresponding diffusion coefficient, is also directly proportional to the concentration gradient of the reactant produced in the diffusion layer. Therefore, both current and concentration gradient magnitudes are related to the concentration of reactant in the bulk. The exact sensitivity of the concentration gradient technique varies, depending upon the particular redox system, but it is close to the sensitivity achieved by electrometer detection. In addition, this method could be used to study zero net electron electrochemical processes [64]. This method, similar to the orthodox Schlieren optics schemes, provides only universal information about the electrochemical interface. In addition, this simple technique can also detect heat generated at the surface during the chemical process, thus possibly providing important thermodynamic information about the chemical process. This signal can readily be separated from the concentration gradient signal due to the large difference between thermal and mass diffusivities. The temperature gradient will reach the probe beam area first, followed by the concentration gradient.

The most limiting factor of Schlieren optics methods is the fact that the net refractive index gradient above the electrode is produced by opposing concentration gradients related to products and reactants. Investigation of complex electrochemical processes requires the application of selective methods in order to distinguish between various electrochemical species.

The above limitation can be resolved by using the selective concentration gradient method as described above. After excitation of the electrochemical interface by the laser pulse, the relaxation generates non-uniform heating in the system, which then slowly reaches thermal equilibrium. Assuming that the only product of the electrochemical reaction A + e → B and that the electrode surface absorbs at the excitation wavelength, the temperature profile illustrated in Fig. 37 will be generated. Just after the excitation pulse, the temperature is high at the electrode surface and follows the concentration profile of the product in the diffusion layer. Then the whole system relaxes thermally, as shown in Fig. 38. In the deflection experiments the probe beam passes close to the surface of the electrode and probes the fast decay of the thermal gradient. Figure 39 illustrates this point. The initial deflection which is generated just after the excitation pulse, corresponds to the magnitude of the product concentration gradient at the probing dimension. Sometime later, the signal associated
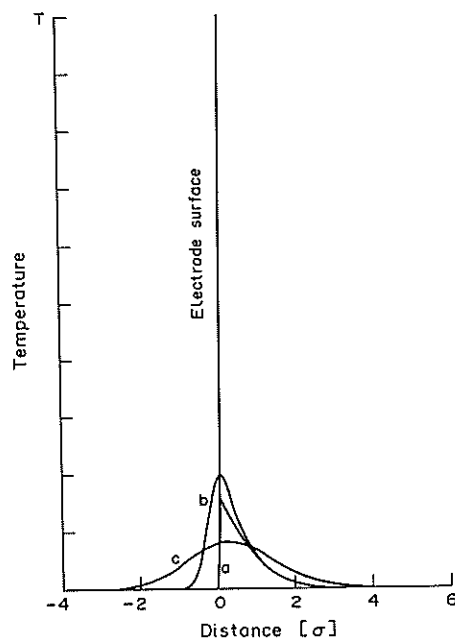
Fig. 37. Temperature profile produced for absorbing electrode surface. Key: (a) just after excitation pulse; (b) after $t = 1/10t_\sigma$ ($t_s = \sigma^2/2D_T$) and (c) after $t = t_\sigma$. The space distance is expressed in $\sigma = (2D_R t)^{1/2}$ units. Adapted with permission from Ref. [36].
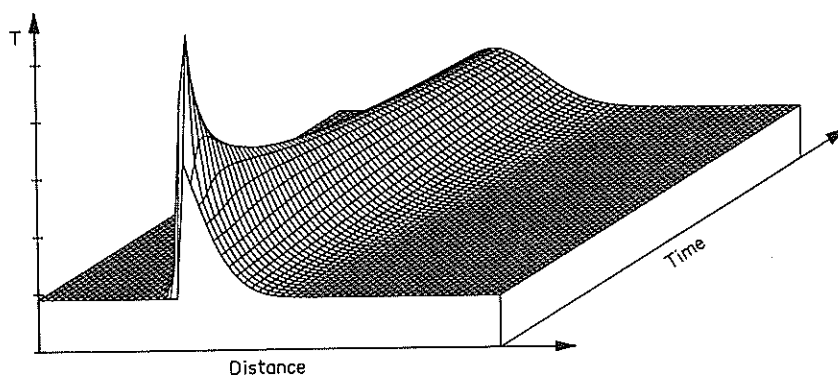

Fig. 38. Axonometric plot illustrating the dynamics of the thermal relaxation process produced for absorbing electrode surface. Adapted with permission from Ref. [36].

with surface absorption will appear. Therefore, it is possible to obtain information about the chemical changes at the electrode surface and the interface simultaneously by carefully analyzing the transient signal [36]. By varying experimental arrangements, it is possible to emphasize information on the surface or at the interface. For example, a solid metal electrode will conduct heat well away from the solution, and therefore the sensitivity of the method to the surface signal will be low. However, if a thin metal electrode is deposited onto a good heat insulator then a significant portion of heat generated at the surface will be transmitted towards the probing beam located in the solution, thus ensuring high sensitivity. On the other hand, the excitation beam can propagate parallel to the electrode surface and effectively eliminate the signal associated with the surface [36].

Spectroscopic characterization of electroactive species is made possible by varying the excitation wavelength and collecting their whole spectra [32]. This will facilitate identification of peaks present in cyclic voltammograms, and enable application of this method to the analysis of real samples.
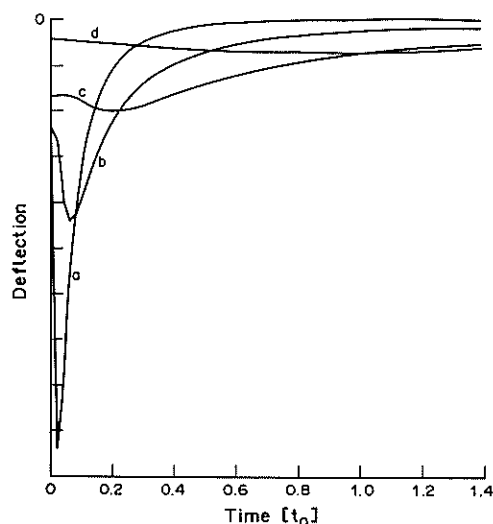
Fig. 39. Transient deflection signal produced after the excitation pulse at a distance of (a) x_0 = $1/4\sigma$; (b) $x_0 = 1/2\sigma$; (c) $x_0 = \sigma$; and (d) $x_0 = 2\sigma$. Time is in t_σ units. Adapted with permission from Ref. [36].

When sensitive and selective imaging techniques based on Schlieren optics are developed, this method can also be used to study the composition of the entire electrochemical interface.

The Schlieren method is more general than electrometer detection, since any process which generates concentration gradients can be investigated, not only those which involve electron transfer from or to the electrode. Therefore any chemical system which involves mass transport (diffusion) and/or mass conversion (chemical reaction) processes can be studied by similar methods developed for electrochemistry using the concentration gradient detection scheme [65].

6.6. Dynamics of chemical processes in liquids

It is well accepted that a better understanding of the dynamics of chemical processes will lead to important breakthroughs in chemistry. The critical nature of these studies illustrate an important fact that, due to kinetic and diffusion limitations, living systems can prosper for extended periods of time in a state far from equilibrium. One of the dynamic problems currently under intensive investigation is chemical oscillation [66, 67], where kinetic rates of elementary chemical reactions and diffusion are coupled together, producing concentration patterns and corresponding gradients in both time and space.

In order to define the dynamics of a given chemical system, one needs to measure mass conversion and/or mass transport rates. For example, for the chemical reaction

$$A + B \rightarrow C \tag{39}$$

we have a differential equation which describes this process:

$$\frac{\partial C_c}{\partial t} = D_C \frac{\partial^2 C_c}{\partial x^2} + k_F C_A C_B - k_R C_c \tag{40}$$

where D_C is a diffusion coefficient of the product C in the medium, while k_F and k_R are the rate constants for the forward and reverse chemical reaction expressed by Eqn (39). Assuming appropriate boundary conditions, the concentration profile can be found analytically by using the Laplace transform method [68]. From this concentration function, the spatial and temporal behaviour of the concentration gradient signal will be obtained. This procedure will allow comparison between the model and experimental

data. The gradient method emphasizes changes in concentration and therefore the dynamics of the system rather than the absolute value or concentration, which emphasizes its static behaviour described by equilibrium constants.

Figure 40 illustrates an experimental arrangement which can be used to study the chemical reactions produced in the diffusion layer above a membrane. Initially, fresh reagent solutions A and B, with matched refractive indices, are introduced in appropriate parts of the cell separated by a membrane. The whole system is then allowed to relax. During this time, the concentration gradients produced above the membrane caused by diffusion and chemical reaction can be measured. Figure 41 summarizes the results obtained in such an experiment. Figure 41a shows the gradients of the Fe–EDTA complex formed during the reaction between Fe^{3+} and EDTA. A single deflection peak is observed for this reaction. The peak height increases as the reagent concentration increases. If a mixture of two metal ions is used (Fig. 41B), two separate peaks are observed. This effect results from significant differences in the equilibrium constants for the formation of the two complexes. The Zn^{2+} reaction is followed by Ca^{2+} complexation some time later, after additional amounts of EDTA diffuse through the membrane [65].

It can be recognized immediately that the approach described above has the potential to become an analytical tool as a microtitration method, especially if selective membranes are used. Moreover, it can also be used as a powerful and simple tool for studying the dynamics of chemical reaction in fluids. The mechanisms can be modelled mathematically and then compared with experimental results in a similar way as has been done for electrochemistry.

The most promising use of Schlieren optics in studying the dynamics of chemical systems involves investigations in multidimensional space, to allow the simultaneous investigation of the evolution of gradient profiles in space and time. In these applications, the single position sensor is replaced by one- and two-dimensional diode arrays (a solid state camera). Three general approaches can be taken to achieve this goal. In the first one, the laser beam is scanned across the object. Application of this
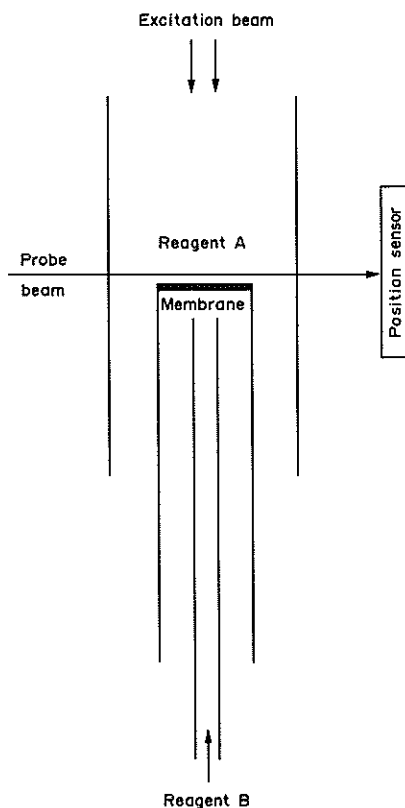

Fig. 40. Experimental arrangement to study chemical reactions in fluids involving membrane.
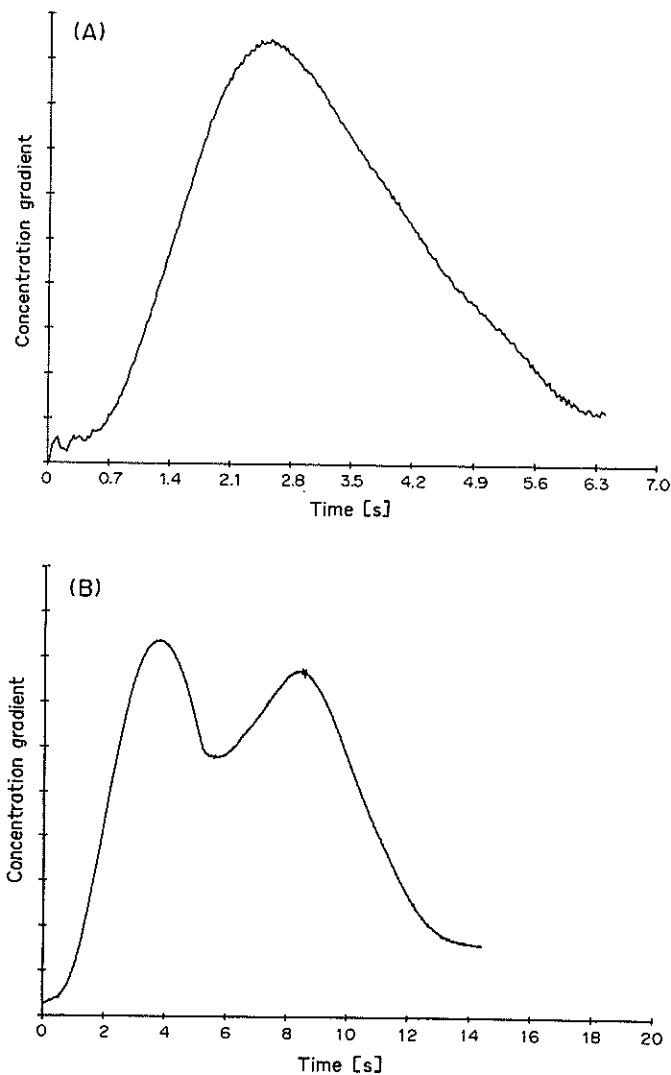
Fig. 41. (A) Typical concentration gradient signal produced by reaction between Fe^{3+} (Reagent A) and EDTA (Reagent B). (B) Concentration gradient signal corresponding to a mixture of Zn^{2+} and Ca^{2+} ions.

method is limited to a single dimension for reasonable acquisition speed. The second one involves the traditional Schlieren–Toepler system already discussed before in this review (Fig. 15). This technique requires good quality, quite complex optics and has difficulty providing good quantitative evaluation of concentration gradients. The third approach involves a shadowgraph system with ray tracing calculations to explain the experimental data. Using this method, it would be possible to study the dynamics of a chemical system without solving differential Eqn (40). The $\dfrac{\partial^2 C_c}{\partial x^2}$ (x,t) component can be measured directly. Also, $\dfrac{\partial C_c}{\partial t}$ (x,t) can easily be computed by knowing initial conditions. The only unknown terms will be the rate constants, which could be obtained by the solving of a series of simultaneous equations related to different species involved in the process.

7. CONCLUSIONS

The concentration gradient method based on Schlieren optics provides:

(1) *In situ* determinations, allowing real time monitoring of chemical processes.
(2) Remote optical sensing, allowing non-interfering monitoring of chemical processes.

(3) High sensitivity measurements capable of detecting femtograms of species which form large concentration gradients.

(4) Spectroscopic selectivity, allowing monitoring of only the selected species forming the gradient during experiments.

(5) Spectroscopic characterization of species on the basis of their absorption properties.

(6) Spatially resolved information (down to μm) about the distribution of species in the system.

(7) Time-resolved information about the changes occurring in the system in real time. The time resolution is limited by the speed of data acquisition.

(8) Low-volume determinations allow analysis of processes occurring in microscopic systems.

The simple optical arrangement of the concentration gradient sensor allows the design of robust and low-volume detection systems. These devices can be built using silicon components exclusively, which enables their incorporation into integrated systems.

Universal response and drift reduction properties of the method are compatible with capillary separation technology which generates large gradients in the detection volume. This sensor can provide simultaneous absorption information about the sample, and possibly fluorescence by detecting light emission orthogonal to the excitation and probing beams. This multimode approach will allow characterization of eluting sample components. This detection scheme can be applied in other separation systems which generate large concentration gradients, such as flow-field fractionation (FFF) and capillary supercritical fluid chromatography. The design of the detection cell for the gradient method is very important as has been extensively discussed above. For example, it can be expected that high sensitivity of detection for FFF will be facilitated by measurement of the concentration gradient along the field direction, where they are the highest, rather than along the direction of flow where they are much lower [69].

The spectroelectrochemical sensor described above can be incorporated in designing selective sensors which combine both the electrochemical and spectroscopic selectivities. This detection scheme can be used to monitor the systems which do not form concentration gradients, since these gradients are generated above the electrode during the redox process.

Rapid improvement in membrane technology, making them very selective systems, can be used effectively as an analytical tool. The concentration gradient sensor measures directly the mass transport of analyte through these systems and therefore it can identify and quantify components of the mixtures. The dynamic versions of static methods such as solvent extraction will significantly increase speed and selectivity of analytical measurements. Additional selectivity can be obtained by taking advantage of the difference in dynamic behaviour of different sample components in reaction with co-reactant.

Multidimensional gradient analysis of the analytical systems involving flowing streams and flames contribute to understanding the processes involved. This approach can also be used effectively as a detection scheme in future analytical methods such as "true" multidimensional separation techniques. This separation can be achieved by simultaneously applying up to three different displacement processes acting at right angles to one another [70]. The separated compounds of the sample would form the concentration gradient fields, which could be detected by the multidimensional Schlieren optics method.

The focus of this review is directed towards concentration gradient methods. However, the selective mode of the techniques based on the photothermal process described above can be used to image the concentration distributions of absorbing species. In this approach, Schlieren optics is replaced by the interferometric detection method and the temporal changes in refractive indices at given dimensions, after an excitation pulse, are measured, which is proportional to the concentration of absorbing

species. The change in the refractive index of the medium due to temperature rise after the excitation pulse and relaxation process can be obtained from Eqn (25):

$$\Delta n = \frac{dn}{dT} T(x) = 2.303 \, Z \frac{I_0 \epsilon_\lambda}{C_p \rho} \frac{dn}{dT} C(x). \tag{41}$$

The refractive index gradients methods can be used effectively as well to guide the light in a well defined way. For example, the gradient fields produced in the GRID lenses [71] facilitate focusing of the light beam passing through them. In addition, the selective approach described above can be used to modify the gradient field by an external light source [72]. This approach might find future applications in signal processing and optical computing.

REFERENCES

[1] A. Toepler, *Ann. Phys. Chem.* **127**, 556 (1866).
[2] A. Bard and L. Faulkner, *Electrochemical Methods*. Wiley, New York (1980).
[3] P. Rieger, *Electrochemistry*. Prentice-Hall, Inc., Englewood Cliffs, NJ (1987).
[4] M. Golay, In *Gas Chromatography 1958*, Ed. D. Desty, p. 36. Butterworths, London (1958).
[5] A. Sa, *Principles of Electronic Instrumentation*, p. 227. Arnold, East Kilbridge, Scotland (1981).
[6] J. Lephardt, In *Transform Techniques in Chemistry*, Ed. P. Griffiths, p. 294. Plenum, New York (1979).
[7] A. Fasanmade and A. Fell, *Anal. Chem.* **61**, 720 (1989).
[8] H. Bauer and S. Lewin, In *Physical Methods of Organic Chemistry*, Ed. A. Weisserger. Interscience, New York (1960).
[9] H. Schardin, *Ergeb.Exacten Naturwiss.* **20**, 303 (1942).
[10] R. Muller, *Advances in Electrochemistry and Electrochemical Engineering*, Eds. P. Delahay and C. Tobias, Vol. 9. Wiley-Interscience, New York (1973).
[11] *CRC Handbook of Chemistry and Physics*, 64th Edn. CRC, Boca Raton, FL (1985).
[12] D. Bershader, In *Modern Optical Methods in Gas Dynamic Research*, Ed. D. Dosanjh, p. 68. Plenum Press, New York (1971).
[13] E. Yeung, In *Detectors for Liquid Chromatography*, Ed. E. Yeung. John Wiley, New York (1986).
[14] L. Foucault, *Ann Obs. (Paris)* **5**, 197 (1859).
[15] W. Merzkirch, *Flow Visualization*. Academic Press, Orlando, FL (1987).
[16] F. Weinberg, *Optics of Flames*. Butterworths, London (1963).
[17] P. Lloyd, *Optical Methods in Ultracentrifugation, Electrophoresis and Diffusion*. Clarendon Press, Oxford (1974).
[18] C. Van Oss, In *Techniques of Surface and Colloid Chemistry and Physics*, Eds R. Good, R. Stromberg and R. Patrick, p. 213. Marcel Derker, Inc., New York (1972).
[19] W. Howes, *Appl. Opt.* **23**, 2449 (1984).
[20] D. Fournier, A. Boccara and J. Badoz, *Appl. Opt.* **21**, 74 (1982).
[21] W. Jackson, N. Amer, A. Boccara and D. Fournier, *Appl. Opt.* **20**, 1933 (1981).
[22] J. Pawliszyn, *Rev. Sci. Instr.* **58**, 245 (1987).
[23] J. Pawliszyn, *Anal. Chem.* **58**, 3207 (1986).
[24] J. Pawliszyn, M. Weber and M. Dignam, *Rev. Sci. Instr.* **56**, 1790 (1985).
[25] J. Pawliszyn, *Anal. Chem.* **60**, 2796 (1988).
[26] V. Dworak, *Ann. Phys. Chem.* **9**, 502 (1880).
[27] R. Noll, C. Haas, B. Weiki and G. Herriger, *Appl. Opt.* **25**, 769 (1986).
[28] J. Trolinger, *Appl. Opt.* **16**, 473 (1979).
[29] J. Hosch and J. Waters, *Appl. Opt.* **16**, 473 (1977).
[30] W. Wollaston, *Philos. Trans. R. Soc. London* **90**, 667 (1800).
[31] H. Siebeneck, D. Koopman and J. Cobble, *Rev. Sci. Inst.* **48**, 997 (1977).
[32] J. Pawliszyn, M. Weber, M. Dignam, A. Mandelis, R. Venter and S.-M. Park, *Anal. Chem.* **58**, 239 (1986).
[33] H. Carslaw and J. Jaeger, *Conduction of Heat in Solids*, p. 459. Clarendon, Oxford (1986).
[34] J. Pawliszyn, *Anal. Chem.* **60**, 766 (1988).
[35] S. Patankar, *Numerical Heat Transfer and Fluid Flow*, p. 54. McGraw-Hill, New York (1980).
[36] J. Pawliszyn, *Anal. Chem.* **60**, 1751 (1988).
[37] K. Mori, T. Imasaka and N. Ishibashi, *Anal. Chem.* **54**, 2034 (1982).
[38] K. Miyaishi, T. Imasaka and N. Ishibashi, *Anal. Chim. Acta* **124**, 381 (1981).
[39] M. Morris and K. Peck, *Anal. Chem.* **58**, 811A (1986).
[40] J. Gordon, R. Leite, R. Moore, S. Porto and J. Whinnery, *Appl. Phys.* **36**, 3 (1965).
[41] J. Whinnery, *Acc. Chem. Res.* **7**, 225 (1974).
[42] J. Harris and N. Dovichi, *Anal. Chem.* **52**, 695A (1980).

[43] A. Rose, R. Vyas and R. Gupta, *Appl. Opt.* **25**, 4626 (1986).

[44] N. Dovichi, T. Nolan and W. Weimer, *Anal. Chem.* **56**, 1700 (1984).

[45] N. Dovichi, *Prog. Anal. Spectrosc.* **11**, 179 (1988).

[46] L. Aamodt and M. Murphy, *J. Appl. Phys.* **54**, 581 (1983).

[47] B. Royce, F. Sanchez-Sinencio, R. Golstein, R. Muratore, R. Williams and W. J. Yim, *Electrochem. Soc.* **129**, 2393 (1982).

[48] H. Houtman and J. Meyer, *Appl. Opt.* **23**, 2178 (1984).

[49] J. Pawliszyn, *Anal. Chem.* **58**, 243 (1986).

[50] J. Pawliszyn, *J. Liq. Chromatogr.* **10**, 3377 (1987).

[51] J. Pawliszyn and K. Chan, *Clinical Application of Capillary Electrophoresis with Concentration Gradient Detection*, 1990 Pitsburgh Conference, New York, NY, March (1990).

[52] F. Everaerts, J. Beckers and T. Verheggen, *Isotachophoresis*. Elsevier, New York, NY (1976).

[53] P. Bocek, M. Deml, P. Gebauer and V. Dolnik, *Analytical Isotachophoresis*. VCH, Weinheim (1988).

[54] S. Hjalmarsson and A. Baldesten, *CRC Crit. Rev. Anal. Chem.* **11**, 260 (1981).

[55] J. Pawliszyn and T. McDonnell, *Anal. Chem.* submitted.

[56] S. Udseth, J. Loo and R. Smith, *Anal. Chem.* **61**, 228 (1989).

[57] J. Pawliszyn, and G. Runde, *Anal. Chem.*, submitted.

[58] D. Honcock and R. Synovec, *Anal. Chem.* **60**, 1985 (1988).

[59] G. Taylor, *Proc. R. Soc. London* **A219**, 186 (1953).

[60] C. Evans, J. Shabushnig and V. McGuffin, *J. Chromatogr.* **459**, 119 (1988).

[61] K. Peck and M. Morris, *J. Chromatogr.* **448**, 193 (1988).

[62] J. Stwart, *Appl. Opt.* **20**, 654 (1981).

[63] J. Pawliszyn, M. Weber, M. Dignam, A. Mandelis, R. Venter and S.-M. Park, *Anal. Chem.* **58**, 236 (1986).

[64] R. Russo, F. McLarnon, J. Spear and E. Cairns, *J. Electrochem. Soc.* **134**, 2783 (1987).

[65] J. Pawliszyn, presented at the 194th National Meeting of the American Chemical Society, New Orleans, LA (1987).

[66] C. Vidal and P. Hanusse, *Int. Rev. Phys. Chem.* **5**, 1 (1986).

[67] C. Zeeman, In *Towards a Theoretical Biology*, Vol. 4. Aldine and Atherton, Chicago (1972).

[68] J. Crank, *The Mathematics of Diffusion*, p. 19. Clarendon Press, Oxford (1975).

[69] K. Caldwell, *Anal. Chem.* **60**, 959A (1988).

[70] J. Giddings, *Anal. Chem.* **56**, 1258A (1984).

[71] "Grin VII" *Appl. Opt.* **27**, 451 (1988).

[72] J. Pawliszyn, *Method and Apparatus for Detecting Universally and Selectively Concentration Gradients, and for Deflecting a Light Beam in a Controlled Fashion*. U.S. Pat. 4, 784, 494 and 4, 940 333.